Published in final edited form as:
Biochemistry. 2011 September 13; 50(36): 7787–7799. doi:10.1021/bi201060c.

Thrombospondin-1 and Angiotensin II Inhibit Soluble Guanylyl Cyclase through an Increase in Intracellular Calcium Concentration

Saumya Ramanathan[†], **Stacy Mazzalupo**[‡], **Scott Boitano**[§], and **William R. Montfort**[*,‡]

[†]Department of Molecular and Cellular Biology, University of Arizona, Tucson, Arizona 85721

[‡]Department of Chemistry and Biochemistry, University of Arizona, Tucson, Arizona 85721

[§]Department of Physiology and The Arizona Respiratory Center, University of Arizona, Tucson, Arizona 85721

Abstract

Nitric Oxide (NO) regulates cardiovascular hemostasis by binding to soluble guanylyl cyclase (sGC), leading to cGMP production, reduced cytosolic calcium concentration ($[Ca^{2+}]_i$) and vasorelaxation. Thrombospondin-1 (TSP-1), a secreted matricellular protein, was recently discovered to inhibit NO signaling and sGC activity. Inhibition of sGC requires binding to cell-surface receptor CD47. Here, we show that a TSP-1 C-terminal fragment (E3CaG1) readily inhibits sGC in Jurkat T cells, and that inhibition requires an increase in $[Ca^{2+}]_i$. Using flow cytometry, we show that E3CaG1 binds directly to CD47 on the surface of Jurkat T cells. Using digital imaging microscopy on live cells, we further show that E3CaG1 binding results in a substantial increase in $[Ca^{2+}]_i$, up to 300 nM. Addition of angiotensin II, a potent vasoconstrictor known to increase $[Ca^{2+}]_i$, also strongly inhibits sGC activity. sGC isolated from calcium-treated cells or from cell-free lysates supplemented with Ca^{2+} remains inhibited, while addition of kinase inhibitor staurosporine prevents inhibition, indicating inhibition is likely due to phosphorylation. Inhibition is through an increase in K_m for GTP, which rises to 834 μM for the NO-stimulated protein, a 13-fold increase over the uninhibited protein. Compounds YC-1 and BAY 41-2272, allosteric stimulators of sGC that are of interest for treating hypertension, overcome E3CaG1-mediated inhibition of NO-ligated sGC. Taken together, these data suggest that sGC not only lowers $[Ca^{2+}]_i$ in response to NO, inducing vasodilation, but is also inhibited by high $[Ca^{2+}]_i$, providing a fine balance between signals for vasodilation and vasoconstriction.

Nitric oxide (NO)[1] regulates numerous vital functions in animal physiology including blood pressure, memory formation, platelet aggregation, angiogenesis and tissue development (1). Dysregulation of NO signaling contributes to cardiovascular disease, difficulties in wound healing, diabetes, asthma, and aging. NO is produced through the conversion of L-arginine to L-citrulline by nitric oxide synthase (NOS) (2, 3) and may function in the same cell where

[*]Corresponding author: William R. Montfort, Department of Chemistry and Biochemistry, University of Arizona, Tucson, Arizona 85721; Tel: (520) 621-1884; Fax: (520) 626-9204; montfort@email.arizona.edu.

SUPPORTING INFORMATION AVAILABLE

Figures S1–S5 and Movie M1 are included in supporting information. This material is available free of charge via the Internet at http://pubs.acs.org.

[1]The abbreviations used are: sGC, soluble guanylyl cyclase; DEA/NO, 2-(N,N-Diethylamino)-diazenolate-2-oxide; TSP-1, thrombospondin-1; FITC, fluorescein isothiocyanate; FACS, fluorescence activated cell sorting; $[Ca^{2+}]_i$, cytosolic calcium concentration; SERCA, sarco/endoplasmic reticulum Ca^{2+} ATPase; Ang II, Angiotensin II; PHA, phytohemoagglutinin; BAPTA-AM, acetoxy-methyl ester derivative of 1,2-bis(o-aminophenoxy)ethane-N,N,N',N'-tetraacetic acid); PKG, cGMP-dependent protein kinase G; GPCR, G-protein coupled receptor; IBMX, 3-isobutyl-1-methylxanthine.

it is produced and/or in nearby cells (autocrine/paracrine signaling). Three isoforms of NOS are found in mammals, endothelial NOS (eNOS), neuronal NOS (nNOS) and inducible NOS (iNOS). Both eNOS and nNOS are regulated by Ca^{2+} through its binding to calmodulin. The primary NO receptor is soluble guanylyl/guanylate cyclase (sGC), a heterodimeric protein of ~150 kDa that binds NO through a ferrous heme. NO binding stimulates cyclase activity, the production of cGMP from substrate GTP and the subsequent amplification of NO-dependent signaling cascades (4–7). In smooth muscle cells, this leads to a reduction in cytosolic calcium concentration ($[Ca^{2+}]_i$) and smooth muscle relaxation, a mechanism closely tied to the regulation of blood pressure. While regulation of NOS is relatively well studied (8), the mechanisms underlying sGC regulation are poorly understood (4).

Recently, thrombospondin-1 (TSP-1), a trimeric extracellular matrix protein of 450 kDa, was discovered to be an inhibitor of NO signaling (9). The NO-stimulated increase in endothelial cell proliferation, migration and adhesion, which are of importance for angiogenesis, wound healing and tumor progression, are potently blocked by TSP-1. TSP-1 also blocks smooth muscle relaxation, leading to vasoconstriction. The mechanisms behind TSP-1 attenuation of NO signaling are not yet known but involve inhibition at multiple steps, including those involving vascular endothelial growth factor receptor-2 (VEGFR2), eNOS, sGC and protein kinase G (PKG) (10, 11). Among these, inhibition of sGC is particularly prominent and the focus of the present investigation.

TSP-1 is a multi-domain protein consisting of a globular N-terminal domain, procollagen homology domain, three thrombospondin structural or properdin-like (type 1) repeats, three EGF-like (type 2) repeats, seven Ca^{2+}-binding (type 3) repeats and a globular C-terminal cell-binding domain (Fig. 1) (12–14). The trimeric form of the protein is stabilized through disulfide bonds located just after the N-terminal domain. TSP-1 interacts with multiple cell surface receptors through each of its domains and elicits a multitude of physiological responses. Through its C-terminal domain, TSP-1 binds to CD47 (also called integrin-associated protein; IAP), which is required for sGC inhibition (9).

CD47 is an ~50 kDa integral-membrane protein expressed in most cell types. It is suspected to traverse the membrane five times, and has an IgV-like extracellular domain and a small alternatively-spliced intracellular domain (15). The two well-characterized ligands of CD47 are signal inhibitory receptor protein α (SIRPα) and TSP-1. The CD47/SIRPα interaction functions to regulate innate immunity and experiments using knockout mice reveal that CD47 could act as a “self” marker since lack of CD47 leads to cells being phagocytosed by macrophages (16). CD47 can be co-immunoprecipitated with G-protein G_i (17) and is implicated in triggering G_i-dependent apoptosis in both breast cancer cells (18) and T lymphocytes (19). This has led to the suggestion that CD47 might be a non-canonical G-protein coupled receptor (GPCR) and that CD47/integrin complexes mimic GPCRs (15, 20). When TSP-1 binds to CD47 at the cell surface there is a decrease in cGMP production due to the reduced ability of NO to stimulate sGC. Full length TSP-1, a peptide derived from the C-terminus of TSP-1 (4N1), and a C-terminal fragment of TSP-1 (E3CaG1) have all been shown to inhibit NO signaling through a reduction in sGC activity (9, 10). Previous studies indicate that TSP-1 inhibition of NO signaling is directly through sGC and not, for example, through inhibition of phosphodiesterases (21, 22). Additionally, 4N1 or 4N1K (modified 4N1) and TSP-1 binding to CD47 have each been shown to increase $[Ca^{2+}]_i$ levels in mast cells (23) and fibroblasts (24).

sGC is a heterodimeric enzyme with one alpha subunit of ~77 kDa and one heme-containing beta subunit of ~70 kDa. Each subunit consists of an N-terminal H-NOX domain, central PAS and coiled-coil domains and a C-terminal catalytic domain (25). Sub-cellular localization (26, 27), dimerization status (28), phosphorylation (29–34), protein-protein

interaction (35–38), *S*-nitrosation (39, 40) and $[Ca^{2+}]_i$ levels (41–43) have all been implicated in sGC regulation. Calcium, nitric oxide and cGMP are intimately associated in controlling numerous cellular functions, especially vascular tone. High $[Ca^{2+}]_i$ levels lead to attenuation of NO-induced cGMP accumulation in transformed HEK 293 cells (41), in primary astrocytes (44) and in primary pituitary gland cells (45), and micromolar calcium concentrations can directly inhibit isolated sGC (41, 42, 46).

Based on the foregoing, we hypothesized that TSP-1 inhibition of sGC was mediated through Ca^{2+} signaling. Here, we show that E3CaG1 binding to Jurkat T cells leads to an increase in $[Ca^{2+}]_i$, and that this pulse is required for inhibition of sGC. We also show that a potent vasoconstrictor, angiotensin II (Ang II), which induces an increase in $[Ca^{2+}]_i$ through GPCR AT_1 (47, 48), also inhibits sGC through a Ca^{2+}-dependent mechanism.

MATERIALS AND METHODS

Materials

FITC-conjugated monoclonal anti-human CD47 antibody (B6H12) and an isotype control antibody were obtained from BD Biosciences (San Jose, CA). Anti-integrin antibodies to αV (P2W7 and 272-17E6) were obtained from Abcam. Ionomycin, thapsigargin, PHA and BAPTA-AM were obtained from Invitrogen (Carlsbad, CA). Fura-2AM was obtained from CalBiochem/EMD Biosciences (San Diego, CA). 2-(N,N-Diethylamino)-diazenolate-2-oxide (DEA/NO) was a kind gift from Dr. Katrina Miranda (University of Arizona). Phosphate-buffered saline (PBS) was prepared as 10 mM KH_2PO_4, 10 mM Na_2HPO_4, 137 mM NaCl, 2.7 mM KCl, pH 7.4. Tris-buffered saline (TBS) was prepared as 10 mM Tris.HCl, 150 mM NaCl, pH 7.4. Krebs buffer was prepared as 25 mM HEPES, 120 mM NaCl, 4.75 mM KCl, 1.44 mM $MgSO_4$, 11 mM glucose, pH 7.4. All other reagents were obtained from Sigma unless otherwise noted.

Cell culture

Sf9 cells were maintained in Grace's Insect Media (Invitrogen) supplemented with 10% fetal bovine serum (Atlanta Biologicals), gentamicin (10 mg/ml) and fungizone (0.25 μg/ml). Jurkat T cells (TIB-152™) were purchased from ATCC. Jurkat T cells lacking CD47 (JinB8, (49)) or integrin β1 (Jurkat A1, (50)) were the kind gift of Dr. David Roberts (NIH). All Jurkat cell lines were maintained in RPMI 1640 (Invitrogen) supplemented with 5% fetal bovine serum (FBS), penicillin (5 mg/ml) and streptomycin (1 mg/ml). Jurkat T cells were maintained below 2×10^6 cells/ml, unless otherwise noted, and were weaned from 5% FBS to serum-free conditions starting 48 h prior to all experiments. 3T3 L1 fibroblasts were the kind gift Dr. Tsu-Shuen Tsao (University of Arizona) and were maintained in DMEM (Invitrogen) supplemented with 10% FBS, penicillin (5 mg/ml) and streptomycin (1 mg/ml). MCF-7 cells were obtained from ATCC (HTB-22™) and maintained in DMEM supplemented with 10% FBS, penicillin (5 mg/ml) and streptomycin (1 mg/ml), and used for experiments within 10 passages after thawing.

Flow cytometry

1×10^6 Jurkat T cells resuspended in stain/wash buffer (PBS supplemented with 0.1% BSA, 0.01% NaN_3), were used per assay condition. Cells were incubated with stain/wash buffer or stain/wash buffer supplemented with E3CaG1 (22 nM) for 1 h at 4 °C and were fixed with 4% paraformaldehyde prior to incubation with FITC-conjugated monoclonal anti-human CD47 antibody or isotype control. Cells were washed with stain/wash buffer to remove unbound antibody followed by addition of 4% paraformaldehyde. One-color flow cytometric analysis was performed at 488 nm using a FACScan flow cytometer (BD Biosciences). The emission fluorescence of FITC-conjugated CD47 antibody was detected using a 530/30

bandpass filter and recorded at a rate of 200–400 events per second for 10,000 events gated on FSC (forward scatter) vs. SSC (side scatter). Data were analyzed using CellQuest PRO software (BD Biosciences). Appropriate electronic compensation was adjusted by acquiring cell populations stained with each dye/fluorophore individually, as well as an unstained control.

To examine increased $[Ca^{2+}]_i$ by flow cytometry, we loaded cells with 5 μM Fluo-3AM in Krebs buffer for 30 min at room temperature with gentle mixing every 10 min. The green fluorescence emission of calcium binding dye Fluo-3 was then analyzed following 488-nm laser excitation on a BD LSRII flow cytometer (Becton Dickinson, Inc.). Buffer or E3CaG1 (2.2–220 nM) was added to cell suspension (2×10^6 cells/500 μl), and data were collected after ten min. Where indicated, cells were incubated with anti-CD47 antibody (B6H12) for 20 minutes prior to the addition of E3CaG1. Data were analyzed using FlowJo (v.7.6.4).

Expression and purification of E3CaG1

Baculoviral vector pAcGP67.coco (COCO), encoding E3CaG1 was kindly provided by Dr. Deane Mosher (University of Wisconsin). Expression and purification were carried out as described (51). Briefly, Sf9 cells were grown at 27 °C and were maintained in Grace's Insect Media supplemented with 10% fetal bovine serum and gentamicin and fungizone. When the cells reached a density of 1×10^6 cells/ml, they were transferred to SF900II media (Invitrogen) and were infected with high titer virus at a multiplicity of infection of 5. Media was collected 65 h post infection. After the His-tagged E3CaG1 was purified by immobilized metal ion affinity chromatography, it was stored at −80 °C in TBS supplemented with 2 mM $CaCl_2$. Protein concentrations were determined by the BCA assay (Thermo Scientific, Rockford, IL) using bovine serum albumin as the standard.

Cloning and transient transfection of human soluble guanylyl cyclase

Primers 5'-ctcagtctcgagatctattcctgatgc-3' and 5'-cagtcaggatccgatgttctgcacgaagc-3' were used to amplify human sGC α1 cDNA (ATCC clone MGC-33150) for cloning into pCMV-3Tag-9 (Clontech, Mountain View, CA) between *Bam*HI and *Hin*dIII sites, yielding a C-terminal myc-tagged protein (vector WM397). Human sGC β1 was cloned into pCMV-3Tag-3A (Clontech) between *Sac*I and *Xho*I sites, yielding a C-terminal FLAG-tagged protein (vector WM434). Primers 5'-gcactcgaggtcatcatcctgctttg-3' and 5'-cactgtgagctcatgtacggatttgtg-3' were used to amplify the cDNA from plasmid pSTBlue1-Huβ1 bearing the human sGC β1 cDNA – a gift from Dr. Alan Nighorn (University of Arizona). The Stratagene QuikChange® Lightning Site-Directed Mutagenesis Kit (Agilent, La Jolla, CA) was used to correct all errors in both plasmids to match CCDS34085.1 (GUCY1A3) and CCDS47154.1 (GUCY1B3) (52). Transfection reagent TurboFect™ (Fermentas, Glen Burnie, MD) was used at a ratio of 20 μg plasmid DNA (1:1 ratio of sGCα:sGCβ) to 25 μl reagent per 10-cm dish of cells at 50% confluency. Cells were harvested by trypsinization 12 h after transfection and the cell pellet was quickly frozen in liquid nitrogen.

sGC immunoprecipitation and activity assays

Transiently transfected MCF-7 cells were trypsinized and resuspended in Krebs buffer. To manipulate $[Ca^{2+}]_i$, cells were incubated with ionomycin (1 μg/ml), thapsigargin (400 nM) and 0.1 mM $CaCl_2$ or vehicle control (DMSO) for 15 min. Cell pellets were lysed into homogenization buffer (50 mM Tris-HCl pH 7.5, 100 mM NaCl, 1 mM EDTA, 1 mM TCEP, 1 mM PMSF, protease inhibitor cocktail (10 μl/ml cell lysate)) using a homogenizer. Lysate was spun at 13000 × g and supernatant was combined with anti-FLAG agarose beads (Sigma, St. Louis, MO) for 1 h, 4 °C, on an Adams™ Nutator Mixer (BD Biosciences). After incubation, beads were washed with TBS and evenly divided into 0.6 ml eppendorf

tubes for the sGC activity assays. Inclusion of equal quantities of immunoprecipitated sGC in each assay condition was confirmed by Western blot analysis (supplemental Fig. S1). Western blots were analyzed on an Odyssey Imaging System (LI-COR) and Image J software was used to analyze loading quantities. Reactions were carried out in a final volume of 100 µl containing reaction buffer (3 mM GTP, 8 mM $MgCl_2$, 50 mM Hepes, pH 7.7, prepared at 10X concentration just prior to use) and, where indicated, 10 µM YC-1 or BAY 41-2272 or vehicle control, and 10 µM DEA/NO. YC-1 and Bay 41-2272 were dissolved in DMSO and then diluted to a final stock concentration of 1.1 mM in ethanol. DEA/NO was prepared as a 1 mM stock solution in 10 mM NaOH. Upon adding DEA/NO or vehicle control, the assay was allowed to proceed for 5 min at 37 °C. The reactions were stopped by pelleting the beads and transferring the supernatant to Cell Lysis Buffer (Molecular Devices, Sunnyvale, CA, or Cisbio, Bedford, MA). cGMP concentrations were determined by competitive ELISA using the CatchPoint™ cGMP assay (Molecular Devices), following the manufacturer's instructions, or the homogenous time resolved fluorescence (HTRF) assay (Cisbio), following the manufacturer's instructions and using a BioTek H1F plate reader.

For kinetic measurements, transiently transfected MCF-7 cells were either treated with DMSO (vehicle control) or ionomycin, thapsigargin and 2 mM $CaCl_2$ for 5 min. Cell pellets were lysed as described above and incubated with anti-FLAG agarose beads for 1.5 hours at 4 °C. Following this, the beads were washed three times and resuspended in an appropriate volume of Tris-buffered saline (pH 7.5). Aliquots of this slurry were then used for activity measurements. Reactions were carried out at 37 °C in a final volume of 150 µl and initiated by the addition of reaction buffer (5–2000 µM GTP, 8 mM $MgCl_2$, 50 mM HEPES, pH 7.5, prepared at 10X concentration just prior to use). Where NO-induced sGC activities were measured, DEA/NO (50 µM) was added immediately after the addition of reaction buffer. Reactions were quenched by the addition of cell lysis buffer from the cGMP kit, generally after 10 min (−NO) or 3 min (+NO). Catalytic rates were linear over these time periods for all GTP concentrations used. Inclusion of equal quantities of immunoprecipitated sGC was confirmed by Western blot analysis (supplemental Fig. S1). For each experiment, cGMP accumulation was measured in duplicate using the cGMP-ELISA kit from Molecular Devices or the HTRF kit from Cisbio; higher concentrations of GTP did not interfere with the measurements. Kinetic parameters were obtained by non-linear fitting of the Michaelis-Menten equation, using SigmaPlot (SPSS, Inc., Chicago). K_m and V_{max} are presented as the average and standard deviation of three independent experiments.

sGC activity and cGMP accumulation in intact cells and cell lysates

Jurkat T cells (1×10^6 per assay condition) were resuspended in Krebs buffer. Where indicated, cells were preincubated with treatment agents (E3CaG1, BAPTA-AM, etc.) or vehicle controls for the indicated time at room temperature, followed by addition of 10 µM DEA/NO. Reactions were stopped after 2 min by placing the cell suspensions on ice, pelleted and quickly frozen. For cGMP measurements, the cell pellets were thawed and resuspended with 100 µL Cell Lysis Buffer. The basal and NO-induced sGC activities of intact cells were expressed in terms of picomoles cGMP produced per minute per milligram of total protein content (pmol cGMP min^{-1} mg^{-1}), using the CatchPoint cGMP assay kit. Protein concentrations were determined by the BCA assay (Thermo Scientific) using bovine serum albumin as the standard.

To examine E3CaG1 inhibition, cells were incubated with 22 nM E3CaG1 in Krebs buffer for 15 min at room temperature, followed by the addition of 10 µM DEA/NO. To manipulate $[Ca^{2+}]_i$, cells were incubated with ionomycin (1 µg/ml) and thapsigargin (400 nM), 20 mM EGTA or vehicle control, and 0–10 mM $CaCl_2$ for 15 min, followed immediately by addition of 10 µM DEA/NO. For experiments examining intracellular

calcium chelation, cells were incubated with BAPTA-AM (10 μM, added from a 2 mM stock solution in DMSO) or vehicle control for 15 min prior to the addition of E3CaG1 (16 nM) or buffer for 15 min, and then DEA/NO (10 μM for 2 min). BAPTA-AM is a membrane permeable Ca^{2+} chelator that is converted to BAPTA in the cytosol, where it becomes trapped.

To examine the effect of PHA or Ang II on sGC activity, Jurkat T cells were grown in serum free media 12 h prior to the experiment at a density of less than 1×10^6 cells/ml. Where indicated, cells were incubated with 5 μM BAPTA-AM or vehicle control (DMSO) for 15 min, followed by the addition of the indicated concentrations of PHA or 1 μM Ang II for an additional 2 min, and then DEA/NO (10 μM) for 2 min. To examine the effect of compounds YC-1 and Bay 41-2272 on E3CaG1 inhibition of sGC, cells were incubated with 22 nM E3CaG1 for 15 min prior to the addition of 10 μM YC-1, 10 μM BAY41-2272 or vehicle control, followed immediately by addition of DEA/NO.

To examine the effect of phosphodiesterases on cGMP accumulation in intact cells, MCF-7 cells transiently transfected with sGC were used. 14 h post-transfection, cells were trypsinized and incubated with vehicle/DMSO, IBMX (0.5 mM) or 8-methoxymethyl IBMX (0.4 mM) for 30 min, followed by addition of ionomycin (1 μg/ml), thapsigargin (400 nM) and calcium chloride (0.1 mM) to appropriate samples, followed immediately by the addition of DEA/NO (10 μM). After 2 min, cells were spun down and cell pellets frozen.

Cell-free inhibition of sGC

MCF-7 cells were transiently transfected with sGC; 14 h post-transfection, cells were trypsinized and pellets were lysed in homogenization buffer. Immunoprecipitation of sGC was performed as described above. Jurkat cell lysate was then incubated with the beads for 15 min at 37 °C with or without 250 nM Ca^{2+} and/or staurosporine (1 μM). Following this, the beads were washed five times with TBS and resuspended in an appropriate volume for activity assay. Where indicated, 10 μM DEA/NO and 10 μM YC-1 were included in the reactions.

sGC activity and cGMP accumulation in lysed Jurkat T cells

25×10^6 Jurkat T cells were used for each assay condition and were incubated with buffer or E3CaG1. Cell pellets were lysed into 600 μl homogenization buffer (50 mM Tris-HCl pH 7.5, 100 mM NaCl, 1 mM EDTA, 1 mM TCEP, 1 mM PMSF, protease inhibitor cocktail (10 μl/ml cell lysate)) using a homogenizer. Lysate was spun at 13000 × g and supernatant was incubated with or without IBMX (0.5 mM) and 8-methoxymethyl IBMX (0.4 mM) for 10 min. This was followed by the addition of Mg-GTP reaction buffer and DEA/NO (10 μM). Reactions were stopped after 2 min by the addition of 250 μl cell lysis buffer (Molecular Devices, Sunnyvale, CA). cGMP concentrations were determined by competitive ELISA using the CatchPoint™ cGMP assay (Molecular Devices), following the manufacturer's instructions.

Calcium imaging

In order to assay $[Ca^{2+}]_i$ in Jurkat T cells, which normally grow in suspension, 3T3 L1 fibroblasts were used to coat glass coverslips with extracellular matrix. Fibroblasts were hypotonically lysed and cellular debris was mechanically removed with a cell scraper. Jurkat T cells were then allowed to adhere to the matrix-coated coverslips. The cells were left undisturbed for a minimum of one hour before use, and remained attached to the coverslips under these conditions for up to four hours. Attached cells were loaded with Fura-2AM for 30 min at room temperature in the dark. Fura-2 fluorescence was observed on an Olympus (Center Valley, PA) IX70 microscope equipped with a 75 W xenon lamp while alternating

between excitation wavelengths of 340 and 380 nm. Images of emitted fluorescence above 505 nm were captured by an ICCD camera (Photon Technology International, Birmingham, NJ) under ImageMaster software control (PTI). Effective $[Ca^{2+}]_i$ was calculated from equations published in (53). Initial $[Ca^{2+}]_i$ was assessed over 20 – 60 s to establish a consistent baseline, and changes in $[Ca^{2+}]_i$ were monitored over time for each experimental condition. Depending on the experiment, measurements were taken every 0.6 sec (for 3 – 5 min experiments) up to 5 s (for experiments > 5 min). Cell morphology within the time period of measurement was assessed by differential interference contrast microscopy, and found not to vary.

Statistical analysis

Data are presented as mean ± S.D of independent experiments. Differences between groups were compared for significance using Student's t-test (calculated with Microsoft Excel software).

RESULTS

CD47 is necessary but insufficient for E3CaG1 binding to Jurkat T cells and inhibition of sGC

To examine the mechanism behind TSP-1 inhibition of sGC, we used E3CaG1, a C-terminal TSP-1 construct that retains robust activity and is more stable than full-length TSP-1. E3CaG1 consists of the last EGFβ-like type II repeat, all of the calcium binding type III repeats and the C-terminal cell-binding domain required for CD47-dependent activity (Fig. 1A). We chose Jurkat T cells for these experiments since these cells are one of the few immortalized cell lines with intact sGC signaling, and since they also respond to TSP-1 (54). Initial experiments with full-length TSP-1 suggested inconsistent inhibition of sGC activity (data not shown). To uncover the reason for this, we used E3CaG1 to study CD47 binding over time. We measured binding of E3CaG1 to Jurkat T cells through its ability to compete with a FITC-conjugated monoclonal anti-human CD47 antibody, using fluorescence activated cell sorting (FACS). We first examined cells that had been kept at low density (0.5×10^6 cells/ml) or that had been cultured for less than 2 weeks. These cells exhibited very little auto-fluorescence and only a small increase in fluorescence upon treatment with a FITC-conjugated isotype control antibody, indicating little non-specific binding occurs. When cells were incubated with the FITC-conjugated CD47 antibody, there was an ~100-fold increase in fluorescence, indicating the presence of CD47 on the surface of Jurkat T cells. Plots of scattering vs. fluorescence for these data ("dot plots", supplemental Fig. S2) indicated a homogenous population of positively stained cells, consistent with a uniform distribution of CD47 throughout the Jurkat T cell population. When E3CaG1 (22 nM) was added to cells prior to the addition of CD47 antibody, the mean fluorescence decreased significantly, indicating that E3CaG1 competes with the monoclonal antibody and binds to CD47 on the Jurkat T cell surface (Fig. 1B). Older cells (> 6 weeks), or cells that had been grown at higher density (3×10^6 cells/ml), could still bind antibody, but E3CaG1 was no longer able to compete with antibody binding (Fig. 1D).

Preparations of E3CaG1 had little effect on the basal activity of sGC in younger cells, but profoundly inhibited NO-stimulated sGC activity (Fig. 1C), much as previously reported in other cell types (9). We observed strong inhibition for E3CaG1 concentrations as low as 0.22 nM (42%, supplemental Fig. S3) and found inhibition to be maximal for concentrations above ~20 nM E3CaG1 (~67%), similarly to previous reports for E3CaG1 and full-length TSP1 (9). Subsequent experiments were performed with 22 nM E3CaG1.

When we examined older Jurkat T cells, no inhibition was seen (Fig. 1E), consistent with the lack of binding as shown in Fig. 1D. We conclude from these experiments that CD47 remains on the cell surface; however, CD47 or a complex that includes CD47 has changed and can no longer interact with the TSP-1 fragment. All subsequent experiments were therefore performed on cells that were within 3 weeks of growth and kept below 1×10^6 cells/ml.

E3CaG1 induces an increase in $[Ca^{2+}]_i$

TSP-1 and peptide 4N1K are known to increase $[Ca^{2+}]_i$ in fibroblasts and mast cells through a mechanism thought to require direct binding to CD47 (23, 24). We hypothesized that E3CaG1 inhibition of sGC in Jurkat T cells also involved changes in $[Ca^{2+}]_i$ and used digital imaging microscopy to examine this possibility (Fig. 2, supplemental movie M1). Jurkat T cells were transferred to matrix-coated coverslips (see Experimental Procedures) for these experiments, and allowed to attach for at least 1 hr, well beyond the time where attachment-associated Ca^{2+} spikes have previously been described, which persist for ~8 min post attachment (55). At rest, Jurkat T cells displayed an $[Ca^{2+}]_i$ of 10 – 25 nM. Addition of E3CaG1 (22 nM final concentration) induced an increase in $[Ca^{2+}]_i$ to 150 – 300 nM (Fig. 2A,B). Similar increases were not observed after washing with Hank's basal salt solution (HBSS, pH 7.4) alone (Fig. 2B). Calcium concentrations could be experimentally controlled within Jurkat cells using the Ca^{2+} chelator BAPTA (Fig. 2C), or the Ca^{2+} ionophore ionomycin and sarco/endoplasmic reticulum Ca^{2+} ATPase (SERCA) pump inhibitor thapsigargin (Fig. 2D). None of the treatment conditions altered cell morphology within the time period of measurement as assessed by differential interference contrast microscopy.

E3CaG1-dependent increases in $[Ca^{2+}]_i$ requires CD47

We examined the requirement for CD47 using flow cytometry and the fluorescent Ca^{2+} indicator Fluo-3. Binding of 2.2 nM or 22 nM E3CaG1 to Jurkat T cells in suspension led to an ~100-fold increase in average fluorescence over addition of buffer alone (Fig. 3A). Thus, Jurkat T cells in suspension behaved similarly to those attached to coverslips. Addition of anti-CD47 antibody B6H12 completely blocked E3CaG1-dependent calcium mobilization. Likewise, cell line JinB8, which is a modified Jurkat T cell lacking CD47 (49), is not sensitive to E3CaG1 (Fig. 3B). Similarly, antibody B6H12 abolishes E3CaG1-dependent inhibition of sGC (Fig. 3C). We conclude that E3CaG1 signaling requires CD47, as expected from previous studies (9). In contrast, antibodies to integrin αV, which is known to associate with CD47 (15), have no effect on E3CaG1-dependent increases in $[Ca^{2+}]_i$ (supplemental Fig. S4) and subsequent inhibition of sGC (Fig. 3C). E3CaG1 also remains active toward cell line Jurkat A1, which are integrin β1 null (data not shown) (50). Additionally, pertussis toxin, which inhibits Gi protein, had no effect on E3CaG1-dependent increases in $[Ca^{2+}]_i$ (supplemental Fig. S4), or on E3CaG1-dependent inhibition of cGMP production (data not shown).

Calcium inhibits NO-inducible sGC activity in Jurkat T cells

Based on previous reports showing that calcium can inhibit sGC activity in HEK 293 cells and also with purified protein (41, 42, 46), we examined whether this was also the case for Jurkat T cells. Jurkat cells were resuspended in Krebs buffer containing 1 μg/ml ionomycin and 400 nM thapsigargin and varying concentrations of extracellular calcium ($[Ca^{2+}]_e$). Under these conditions, $[Ca^{2+}]_i$ is effectively set by $[Ca^{2+}]_e$. NO-inducible cGMP accumulation was inversely proportional to $[Ca^{2+}]_e$ and complete inhibition occurred at $[Ca^{2+}]_e$ = 4 mM (Fig. 4A). Chelating of extracellular calcium with EGTA abolished inhibition. Approximately 99% of cells were viable under each experimental condition, as indicated by trypan blue dye exclusion.

Chelating intracellular Ca^{2+} with compound BAPTA also overcame inhibition of sGC by E3CaG1, indicating that E3CaG1 inhibits sGC through a mechanism requiring increased $[Ca^{2+}]_i$. In the absence of BAPTA, E3CaG1 reduced NO-stimulated cGMP production by 50% (Fig. 4B). However, after pre-loading the cells with BAPTA, E3CaG1 had no effect on cGMP production.

Angiotensin II and phytohemoagglutinin inhibit NO-driven cGMP accumulation

Angiotensin II (Ang II) is a hormone that induces vasoconstriction through binding to GPCR AT_1 and inducing a sustained increase in $[Ca^{2+}]_i$ in targeted cells (47, 48). Phytohemoagglutinin (PHA) is a natural agonist of the T-cell receptor that transiently increases $[Ca^{2+}]_i$ (56). Since Jurkat T cells have Ang II and T-cell receptors (56, 57), we asked whether Ang II and PHA would inhibit cGMP production by sGC. Addition of PHA inhibited NO-stimulated sGC activity in a dose-dependent manner to 60% at the highest concentration examined (50 μg/ml, Fig. 5A). Addition of 1 μM Ang II to cells increased $[Ca^{2+}]_i$ to a similar level as did E3CaG1 (supplementary Fig. S4) and inhibited NO-stimulated sGC activity by 40% (Fig. 5B). As with E3CaG1, chelating intracellular Ca^{2+} with BAPTA reversed this inhibition.

Phosphodiesterases have minimal effect

Previous studies have indicated that TSP1-dependent inhibition of cGMP was through inhibition of sGC and not through stimulation of phosphodiesterases (PDEs) (21, 22). To confirm that this was also true under the conditions of our experiments, we examined cGMP accumulation when PDE was inhibited. We first sought to directly inhibit PDE proteins in live Jurkat T cells using 3-isobutyl-1-methylxanthine (IBMX), a general PDE inhibitor, or 8-methoxymethyl IBMX, a specific inhibitor of calcium/calmodulin-dependent PDE1. Unfortunately, these compounds activate T cells, possibly through a cAMP-dependent mechanism (58), which interferes with the measurement of E3CaG1 activity. We therefore measured NO-dependent cGMP accumulation in Jurkat T cell lysate obtained from cells that were previously treated with E3CaG1 or buffer control; measurements were made in the presence of IBMX or 8-methoxymethyl IBMX (Fig. 6A). Under these conditions, calcium is diluted and PDEs inhibited. Inhibition of NO-stimulated sGC activity was pronounced in the cell-free lysate, consistent with only minor PDE affect on cGMP accumulation.

We further examined the role of PDEs using transiently expressed human sGC in MCF-7 cells, which do not normally express sGC. Raising $[Ca^{2+}]_i$ in these cells led to pronounced inhibition of NO-stimulated sGC activity (Fig. 6B). Addition of IBMX or 8-methoxy IBMX led to small increases in basal, NO-stimulated and calcium-inhibited cGMP levels; however, the 60% reduction in NO-stimulated cGMP accumulation due to increased $[Ca^{2+}]_i$ was unchanged in the presence of these compounds, indicating PDEs have at most a minor role in the observed loss of cGMP under the conditions of our experiments.

Compounds YC-1 and Bay 41-2272 overcome Ca^{2+} inhibition of sGC in live cells

Compounds YC-1 and Bay 41-2272 are small molecule activators of sGC that act synergistically with NO and CO (59); the related compound BAY 63-2521 (Riociguat) is in clinical trial for pulmonary hypertension (60). When included at 10 μM, E3CaG1 inhibition of NO-stimulated sGC was completely overcome by either YC-1 or Bay 41-2272 (Figs. 7A and 7B), suggesting that Ca^{2+} inhibition of sGC is through an allosteric mechanism that can be overcome by allosteric stimulators. YC-1 also inhibits phosphodiesterases (61, 62), which may slightly contribute to the cGMP accumulation shown in Fig. 7A. Although Bay 41-2272 can also inhibit phosphodiesterases (63), inhibition is less pronounced (64, 65) and unlikely to be a factor in Fig. 7B.

Immunoprecipitated sGC remains inhibited, but activity is recovered upon binding compounds YC-1 and Bay 41-2272

That sGC in diluted cell extracts remains inhibited (Fig. 6A) suggests inhibition may be through covalent modification. To further examine this possibility, we transiently expressed human sGC in MCF-7 cells and isolated the protein through immunoprecipitation using a FLAG purification tag. The immunoprecipitated protein displays strong NO-stimulated activity (Fig. 7C). However, when cells were first treated with Ca^{2+}/ionomycin, the isolated protein was substantially inhibited. As with cellular sGC, addition of YC-1 or Bay 41-2272 reversed the inhibition. Thus, higher $[Ca^{2+}]_i$ leads to a modified sGC with reduced activity, and this activity can be overcome by allosteric stimulators.

Two reports indicate that Ca^{2+} can directly inhibit sGC isolated from bovine lung, with K_i values varying between 0.15 and 98.5 μM depending on conditions and laboratory (42, 46). We examined direct inhibition of immunoprecipitated human sGC and found that addition of 100 μM Ca^{2+} led to 50 ± 2% inhibition of the NO-stimulated protein (supplemental Fig. S5) while 1 mM Ca^{2+} brought the sGC activity completely back to basal levels; nanomolar levels of Ca^{2+}, as found in vivo, displayed little inhibition in our hands (data not shown). Neither YC-1 nor Bay 41-2272 was able to overcome direct inhibition by 100 μM Ca^{2+} (supplemental Fig. S5), in contrast to the inhibition of sGC by E3CaG1 in whole cells. The fact that a high concentration of Ca^{2+} is needed to achieve substantial direct inhibition in vitro (micromolar versus nanomolar in the cell), and that YC-1 or Bay 41-2272 do not overcome this inhibition, indicate that direct binding of Ca^{2+} to sGC does not contribute to the observed intracellular sGC inhibition.

Inhibited sGC exhibits an increase in K_m

To further characterize the inhibited sGC, we measured steady-state kinetic parameters for the protein after immunoprecipitation (Fig. 8A, Table 1). The uninhibited protein displayed typical values for K_m and V_{max} (42, 46, 66, 67) and the expected decrease in K_m and increase in V_{max} upon stimulation by NO. In contrast, K_m values for sGC isolated from calcium-treated cells were dramatically increased and unaltered by NO stimulation (Table 1). The inhibited value (K_m ~ 870 μM) is about twice the value for cellular GTP concentrations, which are estimated to be ~470 μM in mammalian tissues (68). At this GTP concentration, the inhibited protein would operate in the cell at well below V_{max}, while the uninhibited protein, with K_m = 67 μM when bound to NO, would be nearly saturated with GTP and operating at near maximal velocity.

Inhibition of sGC requires a calcium-dependent kinase

We developed a cell-free assay for evaluating calcium-dependent inhibition of sGC. Jurkat T cell lysate led to inhibited sGC upon addition of 250 nM Ca^{2+}, but had no effect in its absence (Fig. 8B). Boiling of lysate prior to addition (data not shown), or addition of pan-kinase inhibitor staurosporine (Fig. 8B), prevented inhibition, indicating a calcium-dependent protein kinase was required for inhibition. Obvious candidates for this role are the multifunctional Ca^{2+}/calmodulin-dependent protein kinases I, II and IV. However, addition of compounds KN-62 or KN-93, which inhibit these proteins, had no effect on E3CaG1 inhibition of sGC (data not shown).

DISCSUSSION

The balance between vasoconstriction and vasodilation in mammals, as well as wound healing, angiogenesis and other related activities, relies on the give-and-take of numerous signaling pathways. Here, we reveal a new level of cross regulation: TSP-1 and Ang II, two factors of central importance for cell proliferation and vasoconstriction, can inhibit sGC

activity by increasing $[Ca^{2+}]_i$. The present experiments were performed in Jurkat T cells, a convenient cell line for these studies since the cells perform well in tissue culture, retain endogenous sGC and also respond to TSP-1 and Ang II. This combination is rare in immortalized cells, which in general do not express sGC. Binding of the TSP-1-derived fragment E3CaG1 to CD47 in Jurkat T cells causes free $[Ca^{2+}]_i$ to increase from resting levels of 5–10 nM to peak levels of 300 nM, leading to strong inhibition of sGC (Figs. 1–3). Blocking this increase with chelator BAPTA reverses the sGC inhibition (Fig. 4B). Inducing an increase in $[Ca^{2+}]_i$ with Ang II or PHA (Fig. 5), or with the calcium ionophore ionomycin and SERCA inhibitor thapsigargin (Fig. 4A), also leads to sGC inhibition. These data make clear that Ca^{2+} regulates sGC activity in Jurkat T cells.

The link between Ang II and sGC is particularly interesting to discover. Ang II is part of the renin-angiotensin-aldosterone system for controlling blood pressure through the sensing of blood volume and the linking of kidney function to blood flow (69). The Ang II receptors are G-protein coupled receptors, the most common of which is angiotensin receptor type 1 (AT_1). Binding leads to an increase in $[Ca^{2+}]_i$ through production of inositol triphosphate (IP_3) and subsequent binding to the IP_3-sensitive calcium channel of the sarcoplasmic/endoplasmic reticulum. In vascular smooth muscle, Ca^{2+} stimulates myosin light chain kinase, which phosphorylates myosin, leading to vasoconstriction. Angiotensin converting enzyme (ACE) inhibitors, and AT_1 inhibitors, are commonly used to block this pathway and vasoconstriction in the treatment of hypertension (70). NO-stimulated sGC produces cGMP, which lowers $[Ca^{2+}]_i$ through multiple mechanisms, but in particular *via* phosphorylation of regulatory protein phospholamban by cGMP-dependent protein kinase G (PKG), which leads to stimulation of SERCA and the pumping of Ca^{2+} from the cytosol into cellular stores (71). Interestingly, TSP-1 can also inhibit PKG, further attenuating NO signaling (72). Additionally, fluctuations in $[Ca^{2+}]_i$ may affect the availability of nitric oxide: NADPH oxidase 5 (NOX5), which is found in both vascular smooth muscle and endothelial cells, is stimulated by Ca^{2+} to produce superoxide, a free radical molecule that reacts at the diffusion limit with NO to yield peroxynitrite (73, 74). Thus, our data suggest a feedback mechanism that serves to balance vasodilation through NO and vasoconstriction through Ang II by directly raising and lowering $[Ca^{2+}]_i$ levels (Fig. 9). That this may be the case *in vivo* is supported by a recent study on Ang II-induced hypertension in rats, which demonstrated that Ang II treatment led to blunted sGC activity (75).

A major finding in the present study is that increased $[Ca^{2+}]_i$ leads to inhibition of sGC through covalent modification, most likely by phosphorylation. sGC inhibited in Jurkat T or MCF-7 cells (Figs. 6, 7), or in Jurkat lysate supplemented with 250 nM Ca^{2+} (Fig. 8), remains inhibited after the excess calcium is diluted or washed away, displaying a 13-fold increase in K_{mGTP} in the presence of NO (Fig. 8, Table 1). Inhibition of kinases with staurosporine relieves the calcium-dependent inhibition of sGC (Fig. 8), suggesting inhibition is through direct phosphorylation of sGC. Interestingly, TSP-1-dependent inhibition of PKG also appears to be through covalent modification since inhibition is retained in cell-free extracts (72), indicating a common mechanism may be at work. Although Ca^{2+} can also stimulate Ca^{2+}/calmodulin-dependent phosphodiesterases, particularly in neuronal cell extracts (43), phosphodiesterase activity is at most a minor contributor to the inhibition observed in the present experiments.

sGC allosteric activators YC-1 and Bay 41-2272, which are synergistic with CO and NO for stimulating sGC activity, completely restore NO-stimulated sGC activity. The compounds overcome E3CaG1 inhibition of sGC in Jurkat T cells (Figs. 7A and 7B), and overcome calcium-induced inhibition of sGC in MCF-7 cells (Fig. 7C) or in cell lysate (Fig. 8B). These results suggest the sGC modification leads to a protein that is stabilized in a low activity conformation, but still fully capable of catalysis. Allosteric stimulation by NO alone

is insufficient to drive the modified protein into a fully active state, but in combination with YC-1 or Bay 41-2272, full activity is achieved. Similarly, recent data from Miller and co-workers indicate that stimulation of sGC by YC-1 and Bay 41-2272 in TSP-1 treated platelets and vascular smooth muscle cells is reduced, as was stimulation by NO alone (76); however, stimulation with both YC-1 and NO was not examined in that study. Taken together, these data indicate that both allosteric activator and NO are required to completely overcome TSP-1-dependent inhibition. The data also suggest that the YC-1 class of compounds may offer broad relief to hypertensive individuals, even where Ang II and TSP-1 levels are high, as occurs, for example, in older individuals or those suffering from type-II diabetes (70, 77).

The mechanism by which TSP-1/E3CaG1 causes increases in $[Ca^{2+}]_i$ remains unknown. CD47 is clearly required for signal transduction (Fig. 3). However, E3CaG1 binding is lost as Jurkat T cells age despite the continued presence of CD47 on the cell surface (Fig. 1), suggesting that CD47 alone may not be sufficient for binding and signaling. CD47 was originally identified as integrin associated protein and is likely to function through a signaling complex. Interestingly, CD47 is required for integrin-mediated Ca^{2+} influx in endothelial cells (78), which may be related to the Ca^{2+} signal described herein. Several integrin complexes are known to induce Ca^{2+} influx (79–81), although others reduce $[Ca^{2+}]_i$ (81). CD47 may also associate with G_i protein and thereby function as a non-canonical GPCR (15). In such a mechanism, binding of TSP-1/E3CaG1 would induce Ca^{2+} mobilization through IP_3, much as happens with Ang II binding to AT_1. However, pertussis toxin had no effect on Ca^{2+} mobilization (Fig. S4) or inhibition of sGC in Jurkat T cells, suggesting G_i is not involved, and initial experiments designed to interfere with specific integrins did not alter E3CaG1-dependent Ca^{2+} mobilization (Figs. 3C and S4). Furthermore, TSP-1 transiently decreases IP_3 in A2058 melanoma cells (82).

Finally, it should be noted that autocrine NO signaling, which occurs in endothelial and neuronal cells, is complicated with respect to Ca^{2+}. Increased $[Ca^{2+}]_i$ stimulates eNOS and nNOS, leading to NO production, yet also inhibits sGC. Recent experiments by Isenberg and co-workers using endothelial cells demonstrated that TSP-1 binding through CD47 led to a decrease in the ability of ionomycin to increase $[Ca^{2+}]_i$ and a subsequent decrease in NO production by eNOS (83).

In summary, we have shown that sGC is inhibited by a cellular increase in calcium, which can be induced by extracellular TSP-1 fragment E3CaG1 binding to transmembrane protein CD47 and associated proteins, or by Ang II binding to AT_1. This inhibition of NO-stimulated sGC involves a post-translational modification and can be overcome through the binding of allosteric compounds YC-1 and Bay 41-2272.

Supplementary Material

Refer to Web version on PubMed Central for supplementary material.

Acknowledgments

We are grateful to Deanne Mosher and Doug Annis for generously providing their E3CaG1 expression virus and purification protocols, to Xiaohui Hu for preparing the initial human sGC expression constructs, to David Roberts and Thomas Miller for JinB8 and Jurkat A1 cell lines, and to Jacquie Brailey and Andrzej Weichsel for excellent technical support.

Funding sources: This work was supported by grants from the American Heart Association (09POST2150120 to S.M.), from the National Institutes of Health (T32 HL07249 to S.M., R01 HL062969 and U54 CA143924 to W.R.M., ES 04940 to S.B.) and from the Semiconductor Research Corporation (projects 425.023; 425.024 to S.B.).

Flow cytometry was performed in the AZCC/ARL-Division of Biotechnology Cytometry Core Facility (supported by NIH grant CA023074).

REFERENCES

1. Ignarro, LJ. Nitric Oxide Biology and Pathobiology. San Diego: Academic Press; 2000.
2. Li H, Poulos TL. Structure-function studies on nitric oxide synthases. J. Inorg. Biochem. 2005; 99:293–305. [PubMed: 15598508]
3. Stuehr DJ, Tejero J, Haque MM. Structural and mechanistic aspects of flavoproteins: electron transfer through the nitric oxide synthase flavoprotein domain. FEBS J. 2009; 276:3959–3974. [PubMed: 19583767]
4. Pyriochou A, Papapetropoulos A. Soluble guanylyl cyclase: more secrets revealed. Cell. Signal. 2005; 17:407–413. [PubMed: 15601619]
5. Russwurm M, Koesling D. Guanylyl cyclase: NO hits its target. Biochem. Soc. Symp. 2004; 71:51–63. [PubMed: 15777012]
6. Boon EM, Marletta MA. Ligand specificity of H-NOX domains: from sGC to bacterial NO sensors. J. Inorg. Biochem. 2005; 99:892–902. [PubMed: 15811506]
7. Martin E, Berka V, Tsai AL, Murad F. Soluble guanylyl cyclase: the nitric oxide receptor. Methods Enzymol. 2005; 396:478–492. [PubMed: 16291255]
8. Schulz R, Rassaf T, Massion PB, Kelm M, Balligand JL. Recent advances in the understanding of the role of nitric oxide in cardiovascular homeostasis. Pharmacol. Ther. 2005; 108:225–256. [PubMed: 15949847]
9. Isenberg JS, Ridnour LA, Dimitry J, Frazier WA, Wink DA, Roberts DD. CD47 is necessary for inhibition of nitric oxide-stimulated vascular cell responses by thrombospondin-1. J. Biol. Chem. 2006; 281:26069–26080. [PubMed: 16835222]
10. Isenberg JS, Roberts DD, Frazier WA. CD47: a new target in cardiovascular therapy. Arterioscler. Thromb. Vasc. Biol. 2008; 28:615–621. [PubMed: 18187671]
11. Kaur S, Martin-Manso G, Pendrak ML, Garfield SH, Isenberg JS, Roberts DD. Thrombospondin-1 Inhibits VEGF Receptor-2 Signaling by Disrupting Its Association with CD47. J. Biol. Chem. 2010; 285:38923–38932. [PubMed: 20923780]
12. Bornstein P. Thrombospondins function as regulators of angiogenesis. J. Cell Commun. Signal. 2009; 3:189–200. [PubMed: 19798599]
13. Bonnefoy A, Moura R, Hoylaerts MF. The evolving role of thrombospondin-1 in hemostasis and vascular biology. Cell Mol. Life Sci. 2008; 65:713–727. [PubMed: 18193161]
14. Carlson CB, Lawler J, Mosher DF. Structures of thrombospondins. Cell Mol. Life Sci. 2008; 65:672–686. [PubMed: 18193164]
15. Brown EJ, Frazier WA. Integrin-associated protein (CD47) and its ligands. Trends Cell Biol. 2001; 11:130–135. [PubMed: 11306274]
16. Oldenborg PA, Zheleznyak A, Fang YF, Lagenaur CF, Gresham HD, Lindberg FP. Role of CD47 as a marker of self on red blood cells. Science. 2000; 288:2051–2054. [PubMed: 10856220]
17. Frazier WA, Gao AG, Dimitry J, Chung J, Brown EJ, Lindberg FP, Linder ME. The thrombospondin receptor integrin-associated protein (CD47) functionally couples to heterotrimeric Gi. J. Biol. Chem. 1999; 274:8554–8560. [PubMed: 10085089]
18. Manna PP, Frazier WA. CD47 mediates killing of breast tumor cells via Gi-dependent inhibition of protein kinase A. Cancer Res. 2004; 64:1026–1036. [PubMed: 14871834]
19. Manna PP, Frazier WA. The mechanism of CD47-dependent killing of T cells: heterotrimeric Gi-dependent inhibition of protein kinase A. J. Immunol. 2003; 170:3544–3553. [PubMed: 12646616]
20. Landry Y, Niederhoffer N, Sick E, Gies JP. Heptahelical and other G-protein-coupled receptors (GPCRs) signaling. Curr. Med. Chem. 2006; 13:51–63. [PubMed: 16457639]
21. Isenberg JS, Ridnour LA, Perruccio EM, Espey MG, Wink DA, Roberts DD. Thrombospondin-1 inhibits endothelial cell responses to nitric oxide in a cGMP-dependent manner. Proc. Natl. Acad. Sci. USA. 2005; 102:13141–13146. [PubMed: 16150726]
22. Isenberg JS, Wink DA, Roberts DD. Thrombospondin-1 antagonizes nitric oxide-stimulated vascular smooth muscle cell responses. Cardiovasc. Res. 2006; 71:785–793. [PubMed: 16820142]

23. Sick E, Niederhoffer N, Takeda K, Landry Y, Gies JP. Activation of CD47 receptors causes histamine secretion from mast cells. Cell Mol. Life Sci. 2009; 66:1271–1282. [PubMed: 19205621]
24. Tsao PW, Mousa SA. Thrombospondin mediates calcium mobilization in fibroblasts via its Arg-Gly-Asp and carboxyl-terminal domains. J. Biol. Chem. 1995; 270:23747–23753. [PubMed: 7559547]
25. Poulos TL. Soluble guanylate cyclase. Curr. Opin. Struct. Biol. 2006; 16:736–743. [PubMed: 17015012]
26. Wykes V, Garthwaite J. Membrane-association and the sensitivity of guanylyl cyclase-coupled receptors to nitric oxide. Br. J. Pharmacol. 2004; 141:1087–1090. [PubMed: 15023861]
27. Agulló L, Garcia-Dorado D, Escalona N, Ruiz-Meana M, Mirabet M, Inserte J, Soler-Soler J. Membrane association of nitric oxide-sensitive guanylyl cyclase in cardiomyocytes. Cardiovasc. Res. 2005; 68:65–74. [PubMed: 15953594]
28. Zabel U, Hausler C, Weeger M, Schmidt HH. Homodimerization of soluble guanylyl cyclase subunits. Dimerization analysis using a glutathione s-transferase affinity tag. J. Biol. Chem. 1999; 274:18149–18152. [PubMed: 10373411]
29. Zwiller J, Revel MO, Basset P. Evidence for phosphorylation of rat brain guanylate cyclase by cyclic AMP-dependent protein kinase. Biochem. Biophys. Res. Commun. 1981; 101:1381–1387. [PubMed: 6118147]
30. Zhou Z, Sayed N, Pyriochou A, Roussos C, Fulton D, Beuve A, Papapetropoulos A. Protein kinase G phosphorylates soluble guanylyl cyclase on serine 64 and inhibits its activity. Arterioscler. Thromb. Vasc. Biol. 2008; 28:1803–1810. [PubMed: 18635821]
31. Murthy KS. Activation of phosphodiesterase 5 and inhibition of guanylate cyclase by cGMP-dependent protein kinase in smooth muscle. Biochem. J. 2001; 360:199–208. [PubMed: 11696008]
32. Murthy KS. Inhibitory phosphorylation of soluble guanylyl cyclase by muscarinic m2 receptors via Gbetagamma-dependent activation of c-Src kinase. J. Pharmacol. Exp. Ther. 2008; 325:183–189. [PubMed: 18180373]
33. Ferrero R, Rodriguez-Pascual F, Miras-Portugal MT, Torres M. Nitric oxide-sensitive guanylyl cyclase activity inhibition through cyclic GMP-dependent dephosphorylation. J. Neurochem. 2000; 75:2029–2039. [PubMed: 11032892]
34. Kostic TS, Andric SA, Stojilkovic SS. Receptor-controlled phosphorylation of alpha 1 soluble guanylyl cyclase enhances nitric oxide-dependent cyclic guanosine 5'-monophosphate production in pituitary cells. Mol. Endocrinol. 2004; 18:458–470. [PubMed: 14630997]
35. Russwurm M, Wittau N, Koesling D. Guanylyl cyclase/PSD-95 interaction: targeting of the nitric oxide-sensitive alpha2beta1 guanylyl cyclase to synaptic membranes. J. Biol. Chem. 2001; 276:44647–44652. [PubMed: 11572861]
36. Papapetropoulos A, Zhou Z, Gerassimou C, Yetik G, Venema RC, Roussos C, Sessa WC, Catravas JD. Interaction between the 90-kDa heat shock protein and soluble guanylyl cyclase: physiological significance and mapping of the domains mediating binding. Mol. Pharmacol. 2005; 68:1133–1141. [PubMed: 16024662]
37. Meurer S, Pioch S, Gross S, Muller-Esterl W. Reactive oxygen species induce tyrosine phosphorylation of and Src kinase recruitment to NO-sensitive guanylyl cyclase. J. Biol. Chem. 2005; 280:33149–33156. [PubMed: 16079134]
38. Gambaryan S, Kobsar A, Hartmann S, Birschmann I, Kuhlencordt PJ, Muller-Esterl W, Lohmann SM, Walter U. NO-synthase-/NO-independent regulation of human and murine platelet soluble guanylyl cyclase activity. J. Thromb. Haemost. 2008; 6:1376–1384. [PubMed: 18485089]
39. Sayed N, Baskaran P, Ma X, van den Akker F, Beuve A. Desensitization of soluble guanylyl cyclase, the NO receptor, by S-nitrosylation. Proc. Natl. Acad. Sci. USA. 2007; 104:12312–12317. [PubMed: 17636120]
40. Mayer B, Kleschyov AL, Stessel H, Russwurm M, Munzel T, Koesling D, Schmidt K. Inactivation of soluble guanylate cyclase by stoichiometric S-nitrosation. Mol. Pharmacol. 2009; 75:886–891. [PubMed: 19114587]

41. Parkinson SJ, Jovanovic A, Jovanovic S, Wagner F, Terzic A, Waldman SA. Regulation of nitric oxide-responsive recombinant soluble guanylyl cyclase by calcium. Biochemistry. 1999; 38:6441–6448. [PubMed: 10350462]
42. Serfass L, Carr HS, Aschenbrenner LM, Burstyn JN. Calcium ion downregulates soluble guanylyl cyclase activity: evidence for a two-metal ion catalytic mechanism. Arch. Biochem. Biophys. 2001; 387:47–56. [PubMed: 11368183]
43. Mayer B, Klatt P, Bohme E, Schmidt K. Regulation of neuronal nitric oxide and cyclic GMP formation by Ca2+ J. Neurochem. 1992; 59:2024–2029. [PubMed: 1279121]
44. James LR, Griffiths CH, Garthwaite J, Bellamy TC. Inhibition of nitric oxide-activated guanylyl cyclase by calmodulin antagonists. Br. J. Pharmacol. 2009; 158:1454–1464. [PubMed: 19845679]
45. Andric SA, Kostic TS, Tomic M, Koshimizu T, Stojilkovic SS. Dependence of soluble guanylyl cyclase activity on calcium signaling in pituitary cells. J. Biol. Chem. 2001; 276:844–849. [PubMed: 11031255]
46. Kazerounian S, Pitari GM, Ruiz-Stewart I, Schulz S, Waldman SA. Nitric oxide activation of soluble guanylyl cyclase reveals high and low affinity sites that mediate allosteric inhibition by calcium. Biochemistry. 2002; 41:3396–3404. [PubMed: 11876648]
47. Iversen BM, Arendshorst WJ. ANG II and vasopressin stimulate calcium entry in dispersed smooth muscle cells of preglomerular arterioles. Am. J. Physiol. 1998; 274:F498–F508. [PubMed: 9530266]
48. Kang M, Chung KY, Walker JW. G-protein coupled receptor signaling in myocardium: not for the faint of heart. Physiology. 2007; 22:174–184. [PubMed: 17557938]
49. Ticchioni M, Raimondi V, Lamy L, Wijdenes J, Lindberg FP, Brown EJ, Bernard A. Integrin-associated protein (CD47/IAP) contributes to T cell arrest on inflammatory vascular endothelium under flow. FASEB J. 2001; 15:341–350. [PubMed: 11156950]
50. Romzek NC, Harris ES, Dell CL, Skronek J, Hasse E, Reynolds PJ, Hunt SW 3rd, Shimizu Y. Use of a beta1 integrin-deficient human T cell to identify beta1 integrin cytoplasmic domain sequences critical for integrin function. Mol. Biol. Cell. 1998; 9:2715–2727. [PubMed: 9763439]
51. Mosher DF, Huwiler KG, Misenheimer TM, Annis DS. Expression of recombinant matrix components using baculoviruses. Methods Cell. Biol. 2002; 69:69–81. [PubMed: 12071009]
52. Pruitt KD, Harrow J, Harte RA, Wallin C, Diekhans M, Maglott DR, Searle S, Farrell CM, Loveland JE, Ruef BJ, Hart E, Suner MM, Landrum MJ, Aken B, Ayling S, Baertsch R, Fernandez-Banet J, Cherry JL, Curwen V, Dicuccio M, Kellis M, Lee J, Lin MF, Schuster M, Shkeda A, Amid C, Brown G, Dukhanina O, Frankish A, Hart J, Maidak BL, Mudge J, Murphy MR, Murphy T, Rajan J, Rajput B, Riddick LD, Snow C, Steward C, Webb D, Weber JA, Wilming L, Wu W, Birney E, Haussler D, Hubbard T, Ostell J, Durbin R, Lipman D. The consensus coding sequence (CCDS) project: Identifying a common protein-coding gene set for the human and mouse genomes. Genome Res. 2009; 19:1316–1323. [PubMed: 19498102]
53. Grynkiewicz G, Poenie M, Tsien RY. A new generation of Ca2+ indicators with greatly improved fluorescence properties. J. Biol. Chem. 1985; 260:3440–3450. [PubMed: 3838314]
54. Isenberg JS, Annis DS, Pendrak ML, Ptaszynska M, Frazier WA, Mosher DF, Roberts DD. Differential interactions of thrombospondin-1, -2, and -4 with CD47 and effects on cGMP signaling and ischemic injury responses. J. Biol. Chem. 2009; 284:1116–1125. [PubMed: 19004835]
55. Schottelndreier H, Potter BV, Mayr GW, Guse AH. Mechanisms involved in alpha6beta1-integrin-mediated Ca(2+) signalling. Cell. Signal. 2001; 13:895–899. [PubMed: 11728829]
56. Fischer BS, Qin D, Kim K, McDonald TV. Capsaicin inhibits Jurkat T-cell activation by blocking calcium entry current I(CRAC). J. Pharmacol. Exp. Ther. 2001; 299:238–246. [PubMed: 11561085]
57. Apostolakis S, Vlata Z, Vogiatzi K, Krambovitis E, Spandidos DA. Angiotensin II up-regulates CX3CR1 expression in THP-1 monocytes: impact on vascular inflammation and atherogenesis. J. Thromb. Thrombolysis. 2010; 29:443–448. [PubMed: 19915801]
58. Haubert D, Weckbecker G. Vav1 couples the T cell receptor to cAMP response element activation via a PKC-dependent pathway. Cell Signal. 2010; 22:944–954. [PubMed: 20138987]

59. Evgenov OV, Pacher P, Schmidt PM, Hasko G, Schmidt HH, Stasch JP. NO-independent stimulators and activators of soluble guanylate cyclase: discovery and therapeutic potential. Nat. Rev. Drug Discov. 2006; 5:755–768. [PubMed: 16955067]
60. Mittendorf J, Weigand S, Alonso-Alija C, Bischoff E, Feurer A, Gerisch M, Kern A, Knorr A, Lang D, Muenter K, Radtke M, Schirok H, Schlemmer KH, Stahl E, Straub A, Wunder F, Stasch JP. Discovery of riociguat (BAY 63–2521): a potent, oral stimulator of soluble guanylate cyclase for the treatment of pulmonary hypertension. ChemMedChem. 2009; 4:853–865. [PubMed: 19263460]
61. Friebe A, Mullershausen F, Smolenski A, Walter U, Schultz G, Koesling D. YC-1 potentiates nitric oxide- and carbon monoxide-induced cyclic GMP effects in human platelets. Mol. Pharmacol. 1998; 54:962–967. [PubMed: 9855623]
62. Galle J, Zabel U, Hubner U, Hatzelmann A, Wagner B, Wanner C, Schmidt HH. Effects of the soluble guanylyl cyclase activator, YC-1, on vascular tone, cyclic GMP levels and phosphodiesterase activity. Br. J. Pharmacol. 1999; 127:195–203. [PubMed: 10369473]
63. Mullershausen F, Russwurm M, Friebe A, Koesling D. Inhibition of phosphodiesterase type 5 by the activator of nitric oxide-sensitive guanylyl cyclase BAY 41-2272. Circulation. 2004; 109:1711–1713. [PubMed: 15066950]
64. Bischoff E, Stasch JP. Effects of the sGC stimulator BAY 41-2272 are not mediated by phosphodiesterase 5 inhibition. Circulation. 2004; 110:e320–e321. author reply e320-321. [PubMed: 15381669]
65. Stasch J-P, Becker EM, Alonso-Alija C, Apeler H, Gerzer R, Minuth T, Perzborn E, Pleiss U, Schröder H, Schroeder W, Stahl E, Steinke W, Straub A, Schramm M. NO-independent regulatory site on soluble guanylate cyclase. Nature. 2001; 410:212–215. [PubMed: 11242081]
66. Denninger JW, Schelvis JPM, Brandish PE, Zhao Y, Babcock GT, Marletta MA. Interaction of soluble guanylate cyclase with YC-1: Kinetic and resonance Raman studies. Biochemistry. 2000; 39:4191–4198. [PubMed: 10747811]
67. Chang FJ, Lemme S, Sun Q, Sunahara RK, Beuve A. Nitric oxide-dependent allosteric inhibitory role of a second nucleotide binding site in soluble guanylyl cyclase. J. Biol. Chem. 2005; 280:11513–11519. [PubMed: 15649897]
68. Traut TW. Physiological concentrations of purines and pyrimidines. Mol. Cell. Biochem. 1994; 140:1–22. [PubMed: 7877593]
69. Castrop H, Hocherl K, Kurtz A, Schweda F, Todorov V, Wagner C. Physiology of kidney renin. Physiol. Rev. 2010; 90:607–673. [PubMed: 20393195]
70. Shi L, Mao C, Xu Z, Zhang L. Angiotensin-converting enzymes and drug discovery in cardiovascular diseases. Drug Discov. Today. 2010; 15:332–341. [PubMed: 20170743]
71. Traaseth NJ, Ha KN, Verardi R, Shi L, Buffy JJ, Masterson LR, Veglia G. Structural and dynamic basis of phospholamban and sarcolipin inhibition of Ca(2+)-ATPase. Biochemistry. 2008; 47:3–13. [PubMed: 18081313]
72. Isenberg JS, Romeo MJ, Yu C, Yu CK, Nghiem K, Monsale J, Rick ME, Wink DA, Frazier WA, Roberts DD. Thrombospondin-1 stimulates platelet aggregation by blocking the antithrombotic activity of nitric oxide/cGMP signaling. Blood. 2008; 111:613–623. [PubMed: 17890448]
73. Sumimoto H. Structure, regulation and evolution of Nox-family NADPH oxidases that produce reactive oxygen species. FEBS J. 2008; 275:3249–3277. [PubMed: 18513324]
74. Bedard K, Krause KH. The NOX family of ROS-generating NADPH oxidases: physiology and pathophysiology. Physiol. Rev. 2007; 87:245–313. [PubMed: 17237347]
75. Bae EH, Ma SK, Lee J, Kim SW. Altered regulation of renal nitric oxide and atrial natriuretic peptide systems in angiotensin II-induced hypertension. Regul. Pept. 2011; 170:31–37. [PubMed: 21616096]
76. Miller TW, Isenberg JS, Roberts DD. Thrombospondin-1 is an inhibitor of pharmacological activation of soluble guanylate cyclase. Br. J. Pharmacol. 2010; 159:1542–1547. [PubMed: 20233213]
77. Isenberg JS, Frazier WA, Roberts DD. Thrombospondin-1: a physiological regulator of nitric oxide signaling. Cell. Mol. Life Sci. 2008; 65:728–742. [PubMed: 18193160]

78. Schwartz MA, Brown EJ, Fazeli B. A 50-kDa integrin-associated protein is required for integrin-regulated calcium entry in endothelial cells. J. Biol. Chem. 1993; 268:19931–19934. [PubMed: 8376355]

79. Mariko B, Ghandour Z, Raveaud S, Quentin M, Usson Y, Verdetti J, Huber P, Kielty C, Faury G. Microfibrils and fibrillin-1 induce integrin-mediated signaling, proliferation and migration in human endothelial cells. Am. J. Physiol. Cell Physiol. 2010

80. Sjaastad MD, Nelson WJ. Integrin-mediated calcium signaling and regulation of cell adhesion by intracellular calcium. Bioessays. 1997; 19:47–55. [PubMed: 9008416]

81. Davis MJ, Wu X, Nurkiewicz TR, Kawasaki J, Gui P, Hill MA, Wilson E. Regulation of ion channels by integrins. Cell Biochem. Biophys. 2002; 36:41–66. [PubMed: 11939371]

82. Guo N, Zabrenetzky VS, Chandrasekaran L, Sipes JM, Lawler J, Krutzsch HC, Roberts DD. Differential roles of protein kinase C and pertussis toxin-sensitive G-binding proteins in modulation of melanoma cell proliferation and motility by thrombospondin 1. Cancer Res. 1998; 58:3154–3162. [PubMed: 9679984]

83. Bauer EM, Qin Y, Miller TW, Bandle RW, Csanyi G, Pagano PJ, Bauer PM, Schnermann J, Roberts DD, Isenberg JS. Thrombospondin-1 supports blood pressure by limiting eNOS activation and endothelial-dependent vasorelaxation. Cardiovasc. Res. 2010; 88:471–481. [PubMed: 20610415]

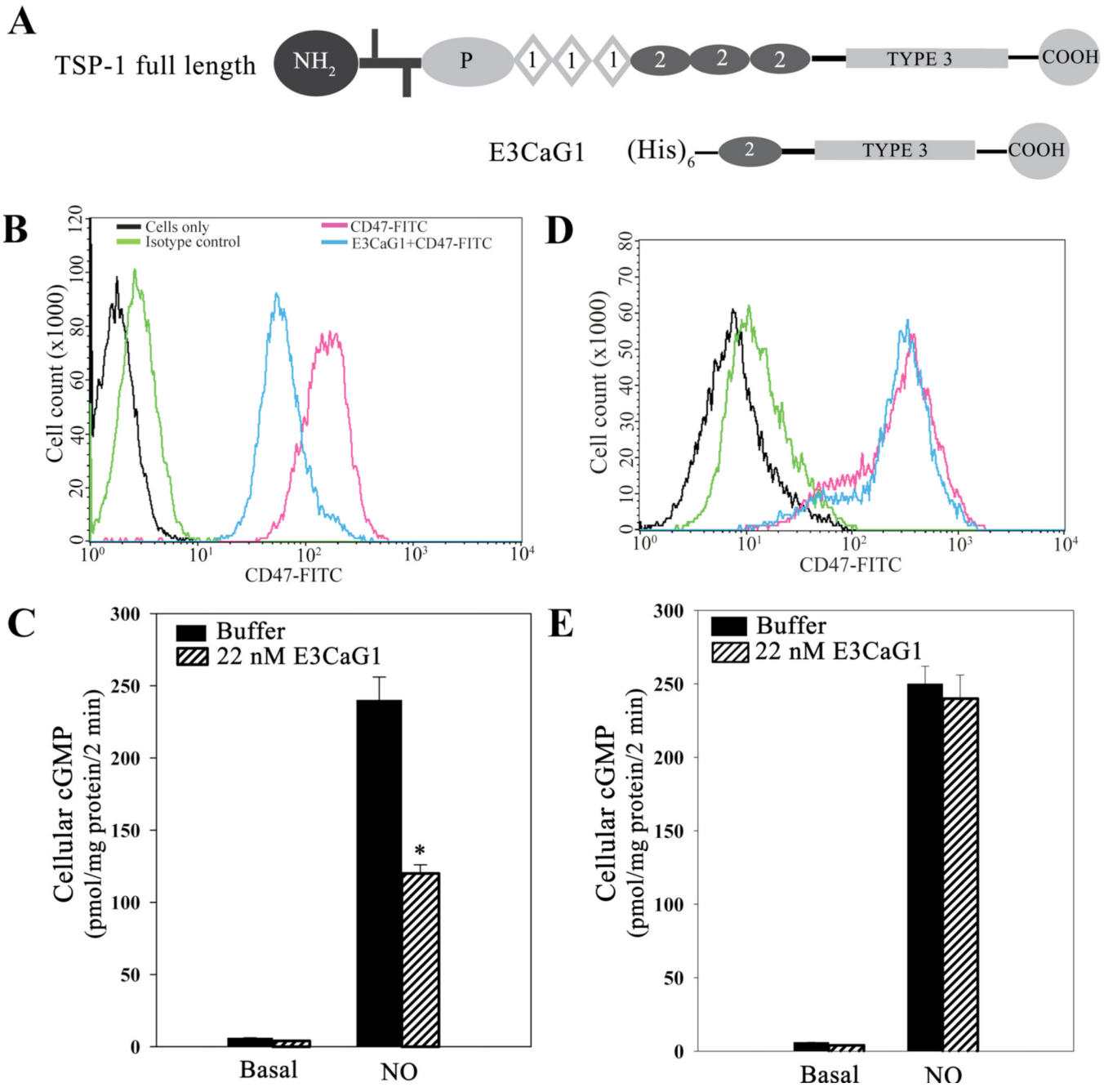

Figure 1.

E3CaG1 binding to Jurkat T cells and inhibition of sGC. *A.* Schematic diagrams of full-length TSP-1 and the recombinant C-terminal fragment used in this study (E3CaG1). N-terminal, C-terminal, procollagen and type 1–3 domains are indicated. Two bars near the N-terminus indicate the cysteines involved in disulfide linkage. *B.* Flow cytometry histogram of Jurkat T cells labeled with FITC-conjugated anti-human CD47 antibody in the presence or absence of E3CaG1, or with isotype or vehicle control, as indicated. 1×10^6 cells were used per condition. Young cells (< 2 weeks in culture) grown at low densities (0.5×10^6 cells/ml) were used; where indicated, cells were incubated with E3CaG1 prior to the addition of the anti-CD47 antibody. *C.* Young Jurkat T cells were examined for cGMP

production (1×10^6 cells per assay condition). Where indicated, cells were incubated with E3CaG1 at room temperature (15 min), followed by the addition of 10 μM DEA/NO. Error bars represent the standard deviation from mean of independent experiments (n = 5) and * denotes $p < 0.001$. *D* and *E* are as in *B* and *C* except that older cells (> 6 weeks in culture), grown to greater densities (3×10^6 cells/ml), were used. Only in the younger cells was E3CaG1 able to compete with binding by the CD47 antibody and inhibit NO-stimulated sGC activity.

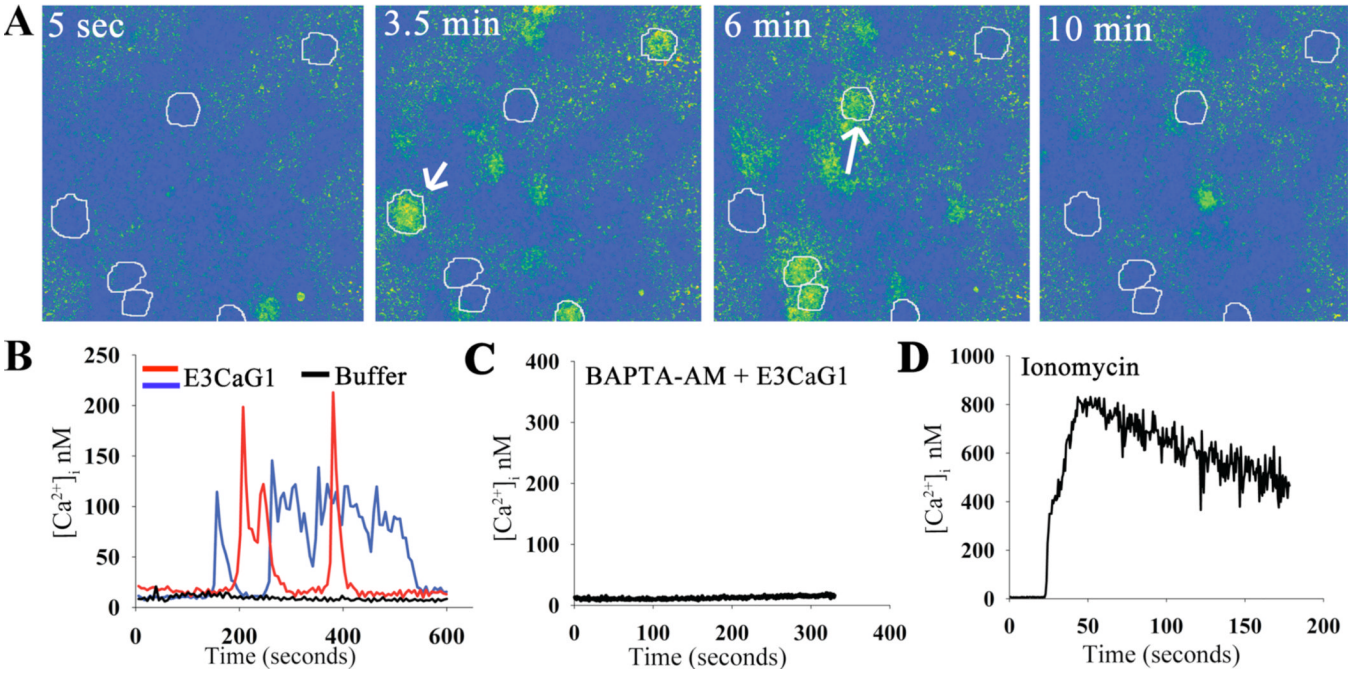

Figure 2.

E3CaG1 induces increase of $[Ca^{2+}]_i$ in Jurkat T cells. Jurkat T cells were attached to coverslips through an extracellular matrix laid down by fibroblasts, and $[Ca^{2+}]_i$ was monitored over time using the calcium indicator Fura-2. *A.* Snapshot of cells in the imaging field at individual timepoints over a 10 min experiment. The coloration indicates $[Ca^{2+}]_i$ after addition of E3CaG1 (22 nM). Six Jurkat T cells of the 40 in the field of view are circled for emphasis. E3CaG1 induced peak $[Ca^{2+}]_i$ in this and similar experiments range from 75 nM up to 300 nM. *B.* $[Ca^{2+}]_i$ traces over time for two representative cells (indicated with arrows in *A*). The black trace represents a typical cell response following addition of the vehicle control (HBSS buffer; from another experiment). *C.* $[Ca^{2+}]_i$ over time of a typical Jurkat T Cell following addition of E3CaG1 (22 nM) after pre-incubation (30 min) with BAPTA-AM (5 μM) to effectively buffer $[Ca^{2+}]_i$. *D.* $[Ca^{2+}]_i$ over time of a typical Jurkat T Cell following addition of 2 mM extracellular $CaCl_2$ in the presence of ionomycin (1 μg/ml) and thapsigargin (400 nM). $[Ca^{2+}]_i$ rises to 800 nM under these conditions.

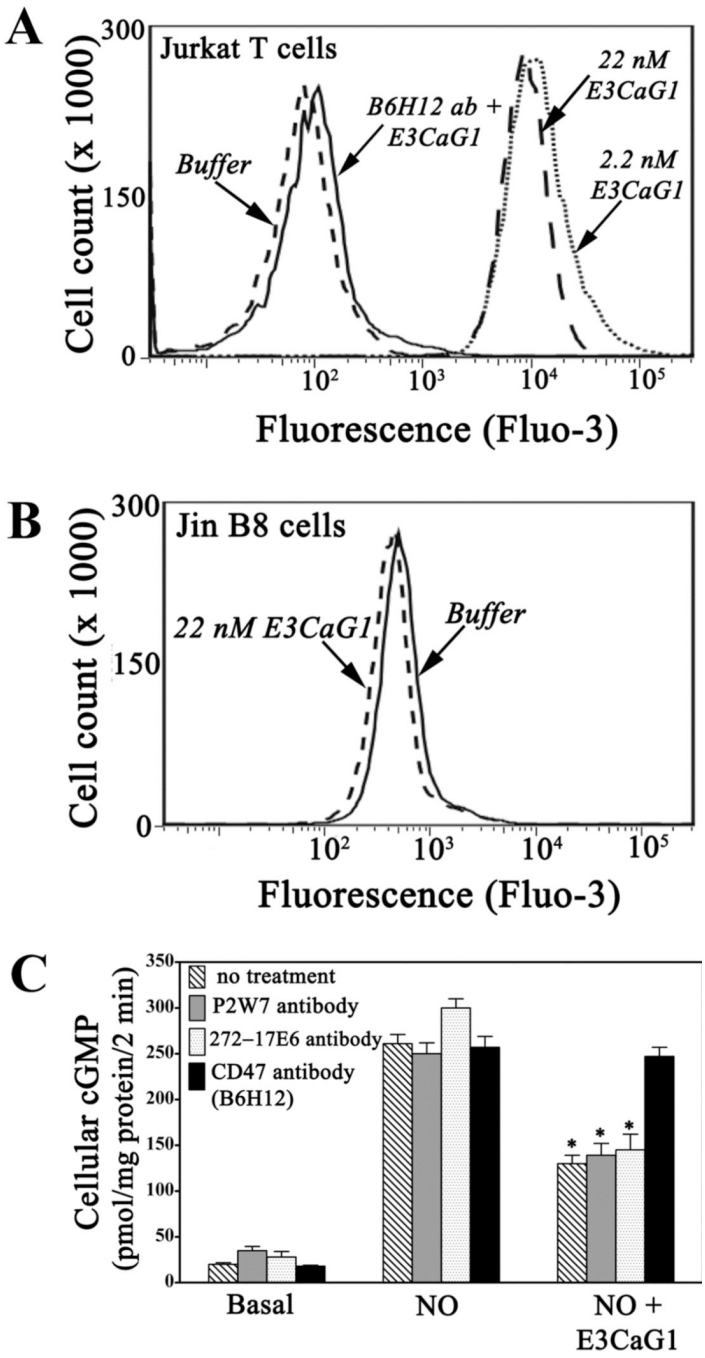

Figure 3.

E3CaG1-induced increases in $[Ca^{2+}]_i$ are cell adhesion independent but require CD47. *A.* Flow cytometry histograms of green fluorescence emission by calcium binding dye Fluo-3. Addition of E3CaG1 (2.2 or 22 nM) to Jurkat T cells results in a 90–100 fold increase in Fluo-3 fluorescence over addition of buffer. Prior incubation with anti-CD47 antibody B6H12 eliminates E3CaG1-dependent increases in $[Ca^{2+}]_i$. *B.* JinB8 cells that lack CD47 do not exhibit increases in intracellular calcium upon addition of E3CaG1. *C.* Addition of anti-CD47 antibody B6H12 prevents E3CaG1-induced inhibition of sGC, whereas addition of anti-integrin αV antibodies P2W7 or 272-17E6 prior to the addition of E3CaG1 does not. Jurkat T cells were incubated with respective antibodies for 30 min at 4 °C prior to the

addition of E3CaG1 (22 nM). After 15 min, 10 mM NaOH (buffer control) or DEA/NO (10 μM) was added as appropriate, followed by incubation for 2 min. Error bars represent the standard deviation from mean of independent experiments (n = 5) and * denotes $p < 0.001$.

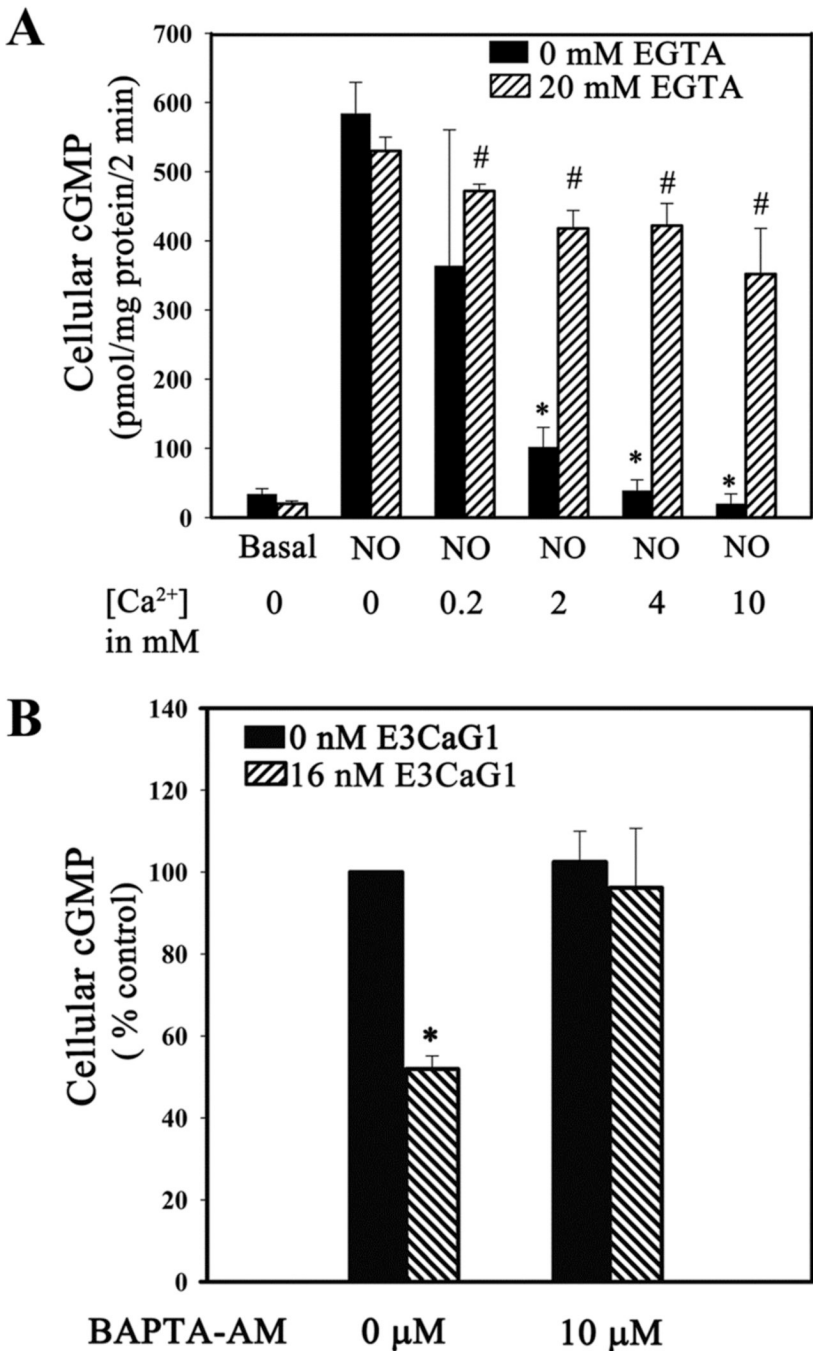

Figure 4.

Increased $[Ca^{2+}]_i$ leads to sGC inhibition in Jurkat T cells. *A.* Manipulation of $[Ca^{2+}]_i$ with ionomycin inhibits sGC. Jurkat T cells (1×10^6) were incubated with the Ca^{2+} ionophore ionomycin (1 μg/ml) and the SERCA-inhibitor thapsigargin (400 nM) for 15 min at room temperature, followed by addition of EGTA (20 mM) or vehicle control, 0–10 mM $CaCl_2$ as indicated, and 10 μM DEA/NO. The reaction was stopped after 5 min. Error bars represent the standard deviation from the mean of independent experiments (n = 5). * denotes $p < 0.001$ and # denotes $p < 0.5$. *B.* Chelating free cytosolic Ca^{2+} with cell permeable chelator BAPTA-AM reverses sGC inhibition by E3CaG1. Jurkat T cells (0.5×10^6) were incubated with 10 μM BAPTA-AM or vehicle control (DMSO) 15 min prior to the addition of

E3CaG1 (16 nM) or buffer and an additional 15 min incubation. This was followed by addition of DEA/NO (10 μM); the reaction was stopped after 2 min. cGMP accumulation was measured and expressed in terms of percentage control (10 μM DEA/NO). Error bars represent the standard deviation from the mean of independent experiments (n = 4), and * denotes $p < 0.001$.

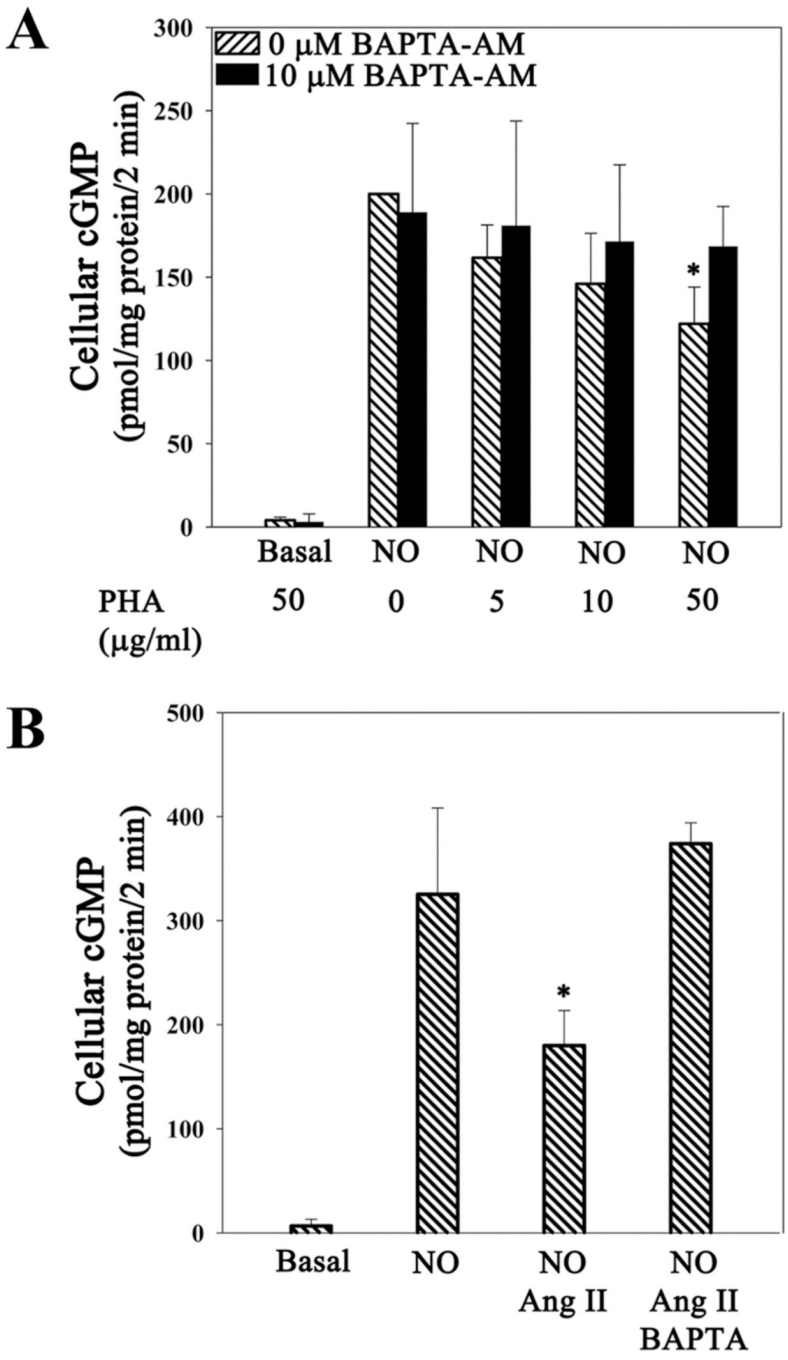

Figure 5.

Stimulation of Ca^{2+} release by Ang II and PHA results in sGC inhibition. Jurkat T cells (0.5×10^6) were incubated with 5 μM BAPTA-AM or vehicle control (DMSO) 15 min prior to the addition of indicated concentrations of PHA, Ang II (1 μM) or buffer and an additional 2 min incubation, followed by addition of DEA/NO (10 μM). The reaction was stopped after 2 min. Both PHA and Ang II inhibited sGC in the absence of BAPTA, but not in its presence. *A.* PHA. *B.* Ang II. Error bars represent the standard deviation from the mean of independent experiments (n = 5), and * denotes $p < 0.01$.

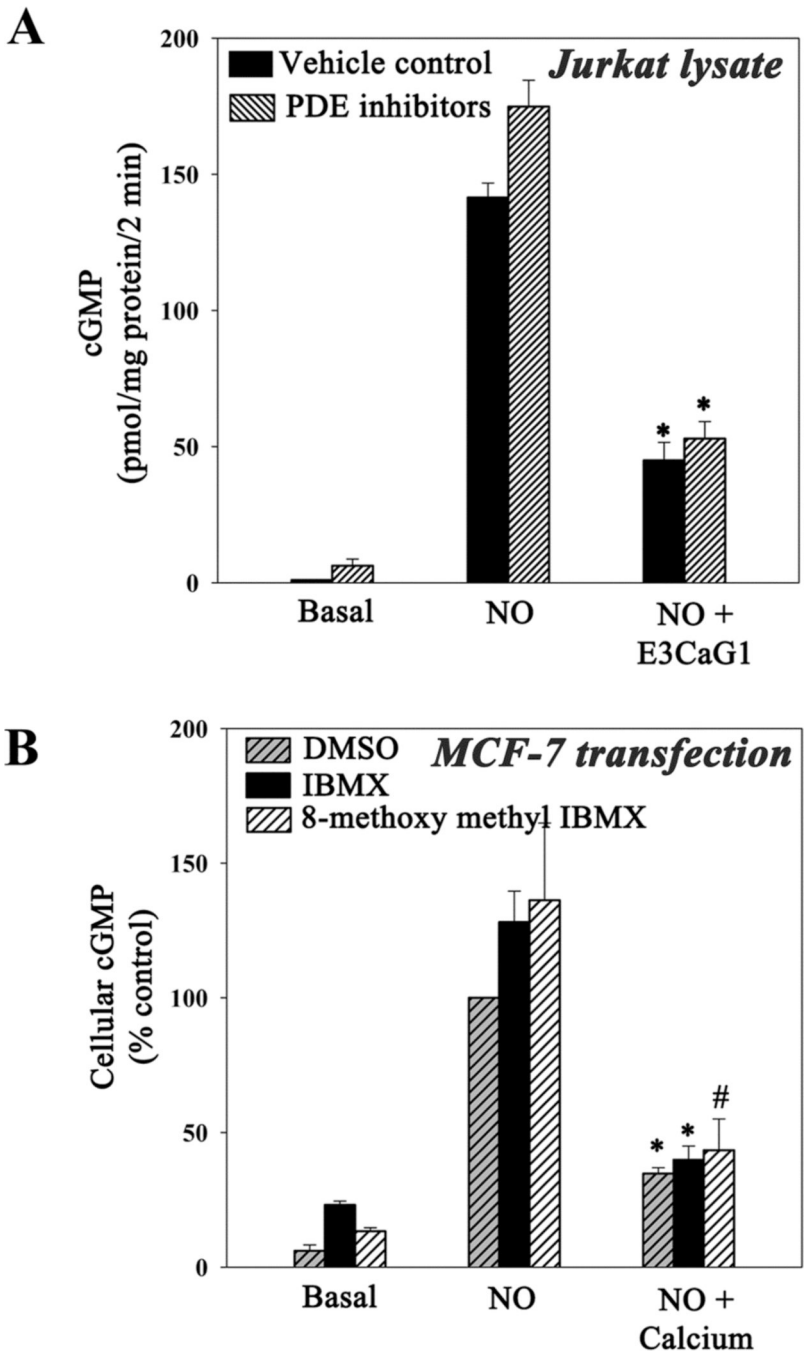

Figure 6.

Phosphodiesterases are minimally involved in Ca^{2+}-dependent lowering of cGMP. *A.* Jurkat T cells (25×10^6) were incubated with 22 nM E3CaG1 or vehicle control (buffer) for 15 min prior to lysis. Lysates were incubated with IBMX (0.5 mM) and 8-methoxymethyl IBMX (0.4 mM) or vehicle control (DMSO) for 10 min. Following this, Mg-GTP reaction buffer and DEA/NO (10 μM) were added and the reaction was stopped after 2 min. Error bars represent the standard deviation from the mean of independent experiments (n = 3), and * denotes $p < 0.001$. *B.* Transiently transfected MCF-7 cells were incubated with IBMX (0.5 mM), 8-methoxymethyl IBMX (0.4 mM) or DMSO (vehicle control) for 30 min followed by addition of ionomycin (1μg/ml), thapsigargin (400 nM) and calcium chloride (0.1 mM) to

appropriate samples, followed immediately by the addition of DEA/NO (10 μM). After 2 min, cells were spun down and cell pellets frozen. cGMP was measured and expressed in terms of percentage control (10 μM DEA/NO). Error bars represent the standard deviation from the mean of independent experiments (n = 3), * denotes $p < 0.001$ and # denotes $p < 0.01$.

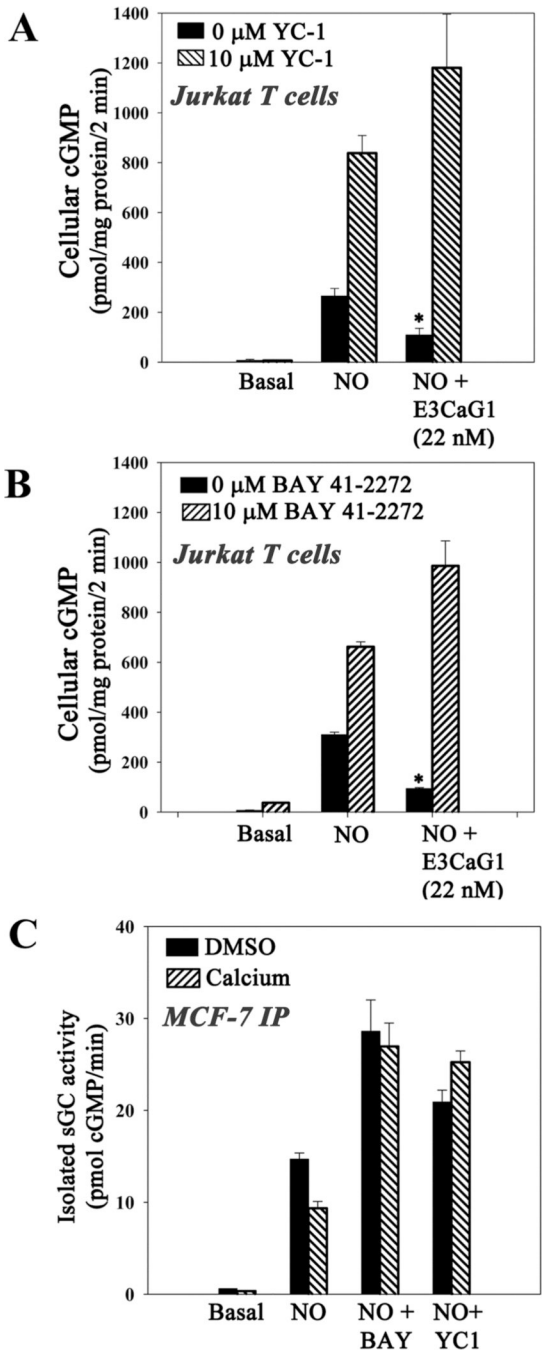

Figure 7.

Compounds YC-1 and Bay 41-2272 overcome Ca^{2+}-dependent inhibition of sGC. *A–B* Jurkat T cells (0.5×10^6) were incubated with 22 nM E3CaG1 or buffer for 15 min prior to the addition of 10 μM YC-1, 10 μM Bay 41-2272 or vehicle control (DMSO). This was followed immediately by the addition of 10 μM DEA/NO. Reactions were stopped after 2 min. Both compounds YC-1 and Bay 41-2272 were able to overcome E3CaG1 inhibition of sGC. *C* Transiently-transfected MCF-7 cells treated with DMSO or 0.1 mM $CaCl_2$ in the presence of ionomycin/thapsigargin. Immunoprecipitated sGC was treated with 10 μM YC-1 or 10 μM Bay 41-2272, followed immediately by the addition of 10 μM DEA/NO. Reactions were carried out at 37 °C for 5 min and cGMP accumulation was measured. Error

bars represent the standard deviation from the mean of independent experiments (n = 5), and * denotes $p < 0.001$.

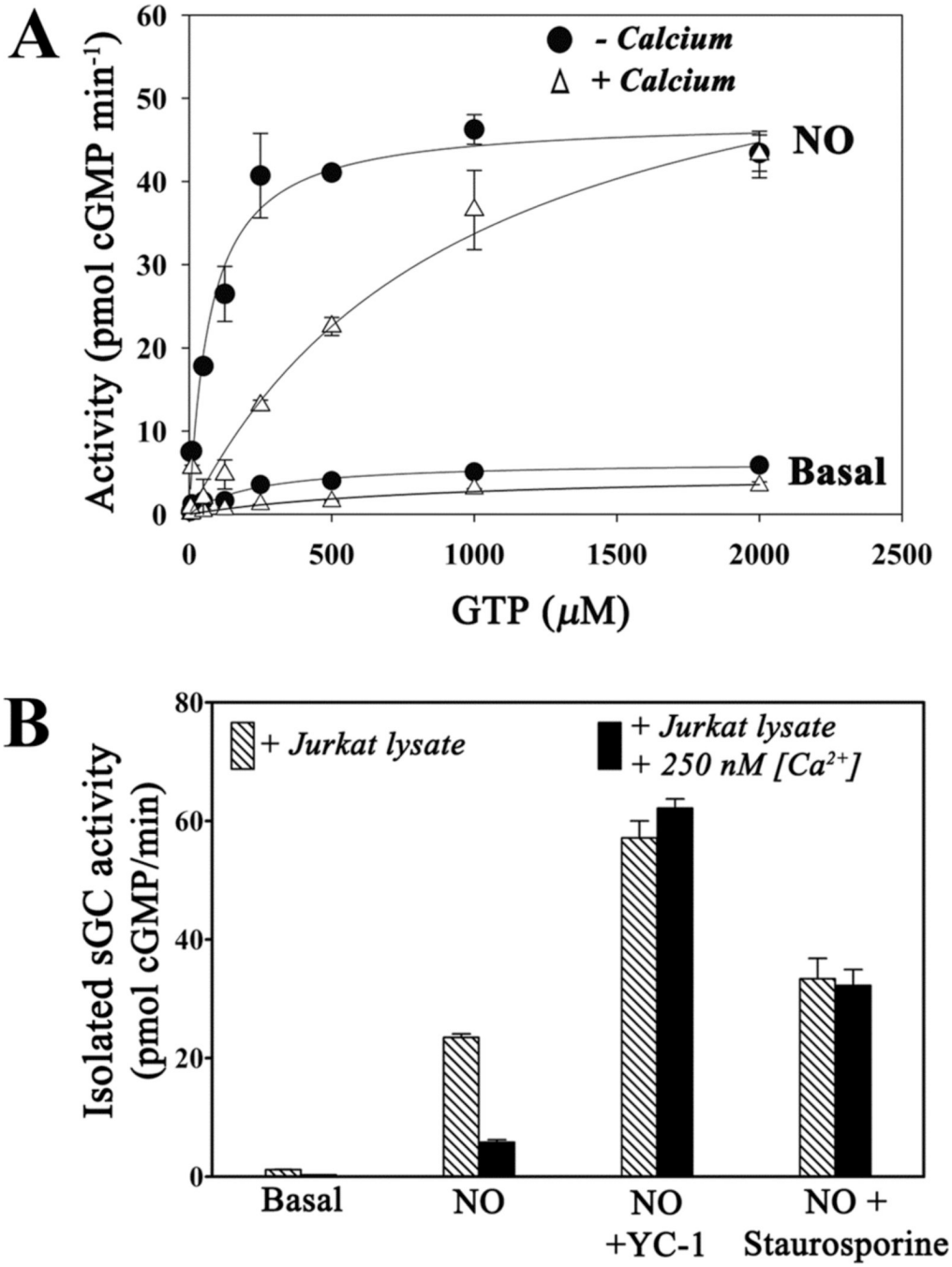

Figure 8.

Representative kinetic plots for immunoprecipitated sGC obtained from MCF-7 cells. Cells were lysed after treatment for 5 min with ionomycin, thapsigargin and 2 mM $CaCl_2$, or vehicle control. Reactions were carried out at 37 °C for 10 min (−NO) or 3 min (+NO). Where included, DEA/NO (50 μM) was added just prior to measurement. Shown are the averages of duplicate measurements ± the range in measured values. The solid curves represent the nonlinear fit to the Michaelis-Menten equation. *B.* Immunoprecipitated sGC treated with Jurkat cell lysate and 250 nM Ca^{2+} is inhibited; inhibition is reversed by broad-range protein kinase inhibitor staurosporine. sGC was immunoprecipitated from transiently transfected MCF-7 cells and incubated with Jurkat T cell lysate with or without 250 nM

Ca^{2+} and/or 1 μM staurosporine. Calcium and staurosporine were washed away and cGMP activity was measured. Where indicated, DEA/NO and YC-1 were added to a final concentration of 10 μM. Error bars represent the standard deviation from the mean of independent experiments (n = 3)

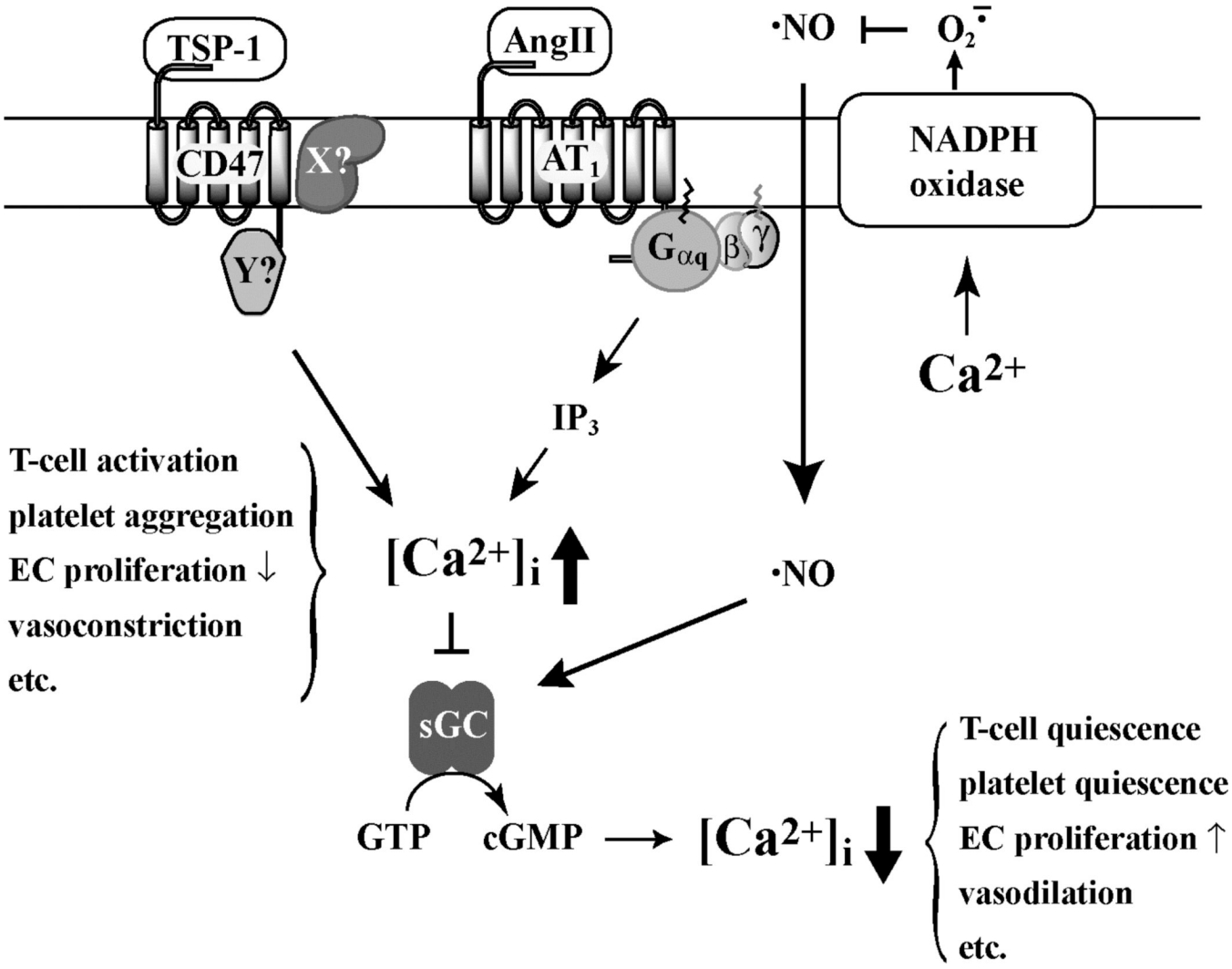

Figure 9.

Proposed model for influence of Ca^{2+} on NO signaling through sGC. Binding of TSP-1 to CD47, or Ang II to AT_1, leads to an increase in $[Ca^{2+}]_i$, which inhibits sGC and stimulates NOX5. The proteins associated with CD47 in the signaling complex are not yet identified, shown here as proteins X and Y. NO-stimulation of sGC leads to a decrease in $[Ca^{2+}]_i$. Changes in $[Ca^{2+}]_i$ may affect T-cell activation, platelet aggregation, endothelial cell (EC) proliferation, vasodilation and other cell and tissue specific physiological responses.

Table 1

Cellular Calcium-Induced Changes in Kinetic Parameters of sGC[a]

	K_{mGTP} (μM)		V_{max} (pmol cGMP min^{-1})[b]		Fold-increase (+Ca^{2+}/−Ca^{2+})[c]	
	−Ca^{2+}	+Ca^{2+}	−Ca^{2+}	+Ca^{2+}	K_m	V_{max}
sGC	234 ± 16	857 ± 31[d]	6.3 ± 1.4	5.1 ± 0.3[d]	3.7	0.8
+NO	69 ± 6	887 ± 71	41 ± 9	51 ± 16	12.9	1.2

[a] Values obtained for immunoprecipitated sGC from MCF-7 cells. Ionomycin, thapsigargin and 2 mM $CaCl_2$, or vehicle control, was added to the cells 5 min prior to lysis.

[b] Presented as pmol min^{-1} since the quantity of sGC protein attached to the anti-FLAG agarose beads is unknown. Total lysate protein was ~65 μg per sample.

[c] Presented as the ratio of +Ca^{2+}/−Ca^{2+} values.

[d] This value is the average ± range of two independent experiments performed in duplicate. All other values are the average ± standard deviation of three independent experiments performed in duplicate.